

## RESEARCH ARTICLE



# Return and volatility transmission between China's and international crude oil futures markets: A first look

Jian Yang<sup>1</sup> | Yinggang Zhou<sup>2,3</sup>

<sup>1</sup>J.P. Morgan Center for Commodities, The Business School, University of Colorado Denver, Denver, Colorado

<sup>2</sup>Center for Macroeconomic Research, Department of Finance, School of Economics (SOE), Xiamen University, Xiamen, China

<sup>3</sup>Wang Yanan Institute for Studies in Economics (WISE), Xiamen University, Xiamen, China

## Correspondence

Yinggang Zhou, Center for Macroeconomic Research, Department of Finance, School of Economics, Xiamen University, Xiamen 361005, China; Wang Yanan Institute for Studies in Economics, A403 Economics Building, Xiamen University, Xiamen 361005, China. Email: [yinggang.zhou@gmail.com](mailto:yinggang.zhou@gmail.com)

## Funding information

National Natural Science Foundation of China, Grant/Award Numbers: 71571106, 71871195, 71988101

## Abstract

We examine return and volatility transmission between the newly established crude oil futures in China and international major crude oil futures markets using intraday data. For the first time, we document evidence for cointegration relationships among these oil futures markets. Both China's and Oman's oil futures markets react to deviations from their long-run equilibrium with West Texas Intermediate and Brent oil futures. There is also new evidence for asymmetric volatilities and correlations across these oil futures markets. Furthermore, the Chinese oil futures have stronger linkages with the international major futures markets than Oman futures.

## KEYWORDS

asymmetry, cointegration, conditional correlation, oil futures

## JEL CLASSIFICATION

E44; G12; G15

## 1 | INTRODUCTION

As of 2018, the crude oil futures markets have been dominated by two international parties: West Texas Intermediate (WTI) in the U.S. and Europe's Brent crude.<sup>1</sup> Despite being the world's largest and fastest-growing oil consumer, Asia, at this point in time, has lacked a leading crude oil futures market.<sup>2</sup> Previous attempts to establish a crude oil futures market have been made in Singapore, Japan, India, and Dubai, but have ultimately been discontinued or thinly traded; the exception is the crude oil futures market in Dubai. In particular, the Dubai Mercantile Exchange's Oman futures market reflects, to a certain extent, the conditions in the Asian market, and is considered to be the regional benchmark for Middle East supplies sold to Asia. However, since its inception in 2007, it has failed to garner great liquidity, indicating that it is not frequently used among market participants.

<sup>1</sup>WTI is the main benchmark for the U.S. crude grades and a crucial hedging tool for its oil industry. Brent, priced off North Sea oil, is the primary value marker for European, the Middle Eastern, and African crudes.

<sup>2</sup>According to the U.S. Energy Information Administration (EIA), Asia and Oceania accounted for 35% of global demand for oil and other liquid fuels in 2017, up from just 30% in 2008.

On March 26, 2018, China launched its yuan-denominated crude oil futures contract on the Shanghai International Energy Exchange (INE), a subsidiary of Shanghai Futures Exchange. Reasons to launch the contract include the increasingly urgent need for China to establish a contract based on supply and demand conditions in Asia as well as mitigating currency risk for Chinese refiners and consumers, as China already overtook the United States in becoming the largest crude oil importer in the world in 2017. It may also be related to China's ambition to augment the global status of the Chinese currency by shifting more global trade into yuan.

The first INE crude oil nearby futures contract with the September 2018 delivery has already seen far more trading than the total amount of the Oman oil futures market during the same period, despite its carrying a small fraction of market shares compared to WTI and Brent. Given China's position in the world economy and its oil consumption, along with the extremely rapid growth of its crude oil futures market (which increased 10-fold in trading volume along with open interest in the first 3 months after its launch), it would be interesting to assess the international linkage between Chinese and international major crude oil futures markets, particularly in light of the INE crude oil futures' goal to become a benchmark in the global crude oil market.

Furthermore, the INE contracts approximate a basket of medium and heavy crudes from the Middle East and China itself with a significantly higher sulfur content, which is close to the underlying crude oil of Oman oil futures contracts in Dubai; both WTI and Brent are based on light low-sulfur crude oils.<sup>3</sup> Thus, China's oil futures market would become the direct competitor with Oman's oil futures market. This would act as China's first step toward becoming an important regional benchmark, reflecting both medium and heavy sour conditions in Asia, before it potentially becomes a global benchmark.

This study examines return and volatility linkages between the Chinese INE futures, the two international major futures markets, Brent and WTI, and its regional competitor in Asia—the Oman futures market in the Middle East. It contributes to the literature in the following aspects.

To our best knowledge, this is the first comprehensive study to explore the long-run price relationship and return and volatility dynamic relationships between the newly launched Chinese crude oil futures and international major crude oil futures markets WTI and Brent. As previous studies (e.g., Lin & Tamvakis, 2001; Liu, Schultz, & Swieringa, 2015) on international linkages of crude oil futures markets primarily focused on the dynamics between WTI and Brent oil futures markets, this study will offer new insights into international crude oil futures market relationships by accounting for both China's and Oman's oil futures markets, which are different from WTI and Brent in terms of the quality of crude oil as the underlying asset.<sup>4</sup>

An equally noteworthy factor is mentioned in Protopapadakis and Stoll's study (1983) in which they point out that an international price relationship for an identical commodity traded across different countries should generally follow the law of one price for a commodity, and such an relationship may be investigated in "its purest form" when commodity futures prices are used. As Chinese commodity futures markets as a whole have become the most actively traded since 2010 (with their exchanges having the highest commodity futures trading volume in the world), there is a growing amount of literature on the linkages of Chinese commodity futures with other global major commodities futures markets: Fung, Leung, and Xu (2003); Fung, Liu, and Tse (2010); Fung, Tse, Yau, and Zhao (2013) examining the information transmission between various Chinese nonoil commodity futures contracts and the corresponding global futures markets, Jiang, Su, Todorova, and Roca (2016) examining the spillovers between the United States and Chinese agricultural futures, and Li and Hayes (2017) investigating price discovery on the Chinese, United States, and Brazilian soybean futures markets.

Crude oil is probably the world's most important and most traded commodity, and with China playing such a crucial role in the world economy, particularly in the commodity markets, this study would fill in an important gap in the literature on international commodity futures market linkages in particular, and international commodity market linkages in general. In our initial findings, we discovered two-way pronounced return and volatility transmissions between international major oil futures and China's oil futures market when the latter was still in its infancy (only 3 months old during the sample period for the baseline analysis). The transmissions displayed stronger results than the case of the Oman oil futures in the Middle East which had existed for over 10 years.

Extending the previous literature, we comprehensively investigated whether all conditional correlations and volatilities show asymmetry across all four international oil futures markets (WTI, Brent, INE, and Oman). Such asymmetry in volatilities and correlations can potentially shed light on the degree of downside risk of international oil futures markets

<sup>3</sup>Both Brent and WTI are classified as a "light sweet" oil blend which means that they are easy to refine compared to heavier and sour oil blends. Specifically, Brent is relatively denser and has a higher sulfur content than WTI.

<sup>4</sup>For example, Lin and Tamvakis (2001) document substantial price spillover effects when both Brent and WTI markets are trading simultaneously, although Brent morning prices are considerably affected by the WTI closing prices of the previous day. Liu et al. (2015) show that there is a decreasing level of cointegration between Brent and WTI markets.

under consideration (e.g., Cappiello, Engle, & Sheppard, 2006). While a few studies (e.g., Kristoufek, 2014; Wang, Wu, & Yang, 2008) have investigated the asymmetric volatility on major international oil futures markets, little has been done on Chinese and Oman crude oil futures markets. Furthermore, despite recent studies using the Dynamic Conditional Correlation (DCC) model (Engle, 2002) to explore correlation dynamics in crude oil and other commodity futures literature (e.g., Chang, McAleer, & Tansuchat, 2011; Hernandez, Ashid, Lemma, & Kuma, 2017), little research has been done to explore the asymmetry in conditional correlations on international oil futures markets linkages in particular, and international commodity futures linkages in general. In this paper, we simultaneously exploit both the asymmetry in volatility and in correlations among the four crude oil futures markets under consideration. We find that China's crude oil futures exhibit stronger asymmetric volatility and correlations than international major oil futures markets.

Finally, we employ a better-quality data set of intraday 5-min high frequency data from both daytime and overnight trading sessions to adequately capture more information transmission across international major crude oil futures markets, which are generally considered to be very liquid with possible new information arrival and absorption within minutes. Recent research has shown that using daily data might not reveal intraday dynamic relationships that are highly relevant in the examination of linkages across oil futures markets and that it might be disadvantageous as the daily closing prices usually only reflect the information at the end of the daytime session without exploiting the information of the overnight session (which is particularly important to the China's crude oil futures market). For example, Kao and Wan (2012) argue that Brent has led WTI in the price discovery process since 2004 due to production, transportation, and inventory bottlenecks in the United States. However, while using intraday data, Elder, Miao, and Ramahander (2014) discover that WTI maintains a dominant role in price discovery relative to Brent. Janzen and Adjemian (2017) make a similar argument for using high frequency intraday data when they explore international linkages of another commodity futures market (i.e., wheat).

Furthermore, by following Janzen and Adjemian (2017), we look at the linkages at different times of day (i.e., daytime vs. overnight sessions) because every market might have different periods of concentrated trading when there is more information production. Interestingly, we find that the linkages between China's and international major crude oil futures are much stronger during the INE overnight session than during the INE daytime trading session. Shanghai International Energy Exchange return is significantly affecting the returns of WTI and Brent futures return only during the INE daytime session, despite there being lower trading volume and open interests during the INE daytime session compared to the INE overnight session.

The rest of the paper is organized as follows: Section 2 describes the data; Section 3 discusses econometric methodology; Section 4 presents empirical results; and Section 5 makes concluding remarks.

## 2 | DATA

### 2.1 | Data description

The prices of two major international oil futures—WTI and Brent—and the newly launched Chinese crude oil futures, recoded at 5-min intervals, are obtained from Bloomberg. The nearby futures contracts are used because they are highly liquid and the most active. While we also have the extended sample period for the additional analysis below, the sample period for the baseline analysis is the first 3 months of the INE oil futures trading from March 26, 2018 to June 26, 2018, as shown in Figure 1. Based purely on physical properties, the INE futures is expected to trade at a discount compared to WTI and Brent since its underlying oil is denser and has a higher sulfur content than WTI and Brent counterparts. Figure 1 demonstrates that the INE oil futures price is between WTI and Brent futures prices and that Brent trades at a substantial premium to WTI and INE. The inversion in the price spread can be attributed to localized factors, such as the dramatic increase in the U.S. oil production. However, there is a general pattern of price comovement between the Chinese futures and the other two futures. Moreover, the INE futures price diverged from the WTI counterpart and converged to the Brent counterpart in the second half of the sample.

The INE opens from 9:00 a.m. to 11:30 a.m., 13:30–15:00, and then from 21:00 p.m. to 2:00 a.m. (Beijing Time) the next day, while the trading hours of the WTI and Brent oil futures contract are 23 hr, from 18:00 to 17:00 next day (New York Time) and 1:00 a.m. to 23:00 (London Time), respectively. After matching overlapping trading hours and exploring 5-min continuous intervals, we obtain a full sample of 6,075 5-min observations of nearby WTI, Brent, and INE oil futures returns during the 3-month sample period, which are calculated by taking first differences of the logarithms of prices.

The underlying crude oil of INE futures is similar to that listed in the Oman Exchange. Therefore, we construct another sample by adding the Oman oil futures. However, further matching only gives 3,744 observations due to limited data on Oman



**FIGURE 1** Prices of WTI, Brent, and INE oil futures. Panel A: Full sample; Panel B: INE daytime trading sample; Panel C: INE overnight trading sample. INE, International Energy Exchange; WTI, West Texas Intermediate

oil futures. We also break the samples into two subsamples of INE daytime trading hours/session and overnight trading hours/session to assess whether the relation between China's oil futures and other markets varies by different time periods of the day.

## 2.2 | Summary statistics

Table 1 reports the summary statistics of oil futures returns. In Panel A, the INE oil futures yielded the average 5-min return of 0.001% in the whole sample and subperiods. In contrast, the average returns of WTI and Brent futures are 0.002% in the whole sample while they are close to zeros during the INE daytime trading and slightly larger than 0.003% during the INE overnight trading. All three oil futures returns are substantially more volatile during the INE nighttime trading period than its daytime trading period, which might be a reflection of more flow of information among these crude oil futures (Ross, 1989), and the INE nighttime trading period overlaps with daytime trading period of WTI and Brent. Among them, China's crude oil futures were more volatile than the WTI and Brent counterparts in the whole sample and the daytime trading subsample. Moreover, crude oil futures were more negatively skewed in the INE than in the WTI and Brent markets. All crude oil futures returns exhibited high kurtosis, which is a very preliminary evidence for higher downside risk of China's crude oil futures during the sample period (to be formally documented below). Brent and INE futures returns were strongly autocorrelated during the daytime of INE trading while serial correlations were quite weak for these two returns. In contrast, WTI oil futures returns were strongly autocorrelated during the nighttime but not during the daytime of INE trading. The squared returns were strongly serial correlated across all three markets under consideration, suggesting the existence of ARCH effects on these markets.

In Panel B of Table 1 for the smaller sample of Oman oil futures, there are very few observations during the INE daytime trading period. In the full sample and INE nighttime trading subsample, Oman oil futures returns were even more volatile and negatively skewed with higher kurtosis compared with the WTI, Brent, and INE counterparts in Panel A. Although serial correlations are very weak for returns of Oman oil futures, its squared returns were strongly serially correlated, which also suggests the existence of volatility clustering.

Panel C of Table 1 shows the correlation matrix of crude oil futures returns. Oil futures returns of nearby WTI and Brent contracts have a high positive correlation in both the full sample and the two subsamples. Also, China's oil futures returns were highly correlated with the WTI and Brent counterparts, yielding the correlations of 78.0% and 78.8% in the full period, respectively. These correlations between the INE and the other two markets are much lower in the INE daytime trading period at 66.4% and 63.7%, while they are somewhat higher in the INE daytime trading period at 79.3% and 80.2%. The difference suggests that China's oil futures market is more integrated with the global market during the nighttime when WTI and Brent futures are traded in their daytime trading. Also, we calculate the correlations between the Oman futures and the other three futures, which are close to zeros and even negative in the full period and the INE overnight trading period.<sup>5</sup>

<sup>5</sup>The correlations between the Oman futures and the other three futures are positive in the INE daytime period. However, the observations are limited in this subsample.

**TABLE 1** Summary statistics of oil futures returns

Panel A: Returns of WTI, Brent, and INE oil futures										
	Stat	Nobs	Mean	SD	Skew	Excess Kurt	Lag1	Lag10	LB Q(10) for return	LB Q(10) for squared return
Whole sample	WTI nearby	6,075	0.002	0.116	−0.748	22.413	−0.016	0.009	25.019***	387.555***
	Brent nearby	6,075	0.002	0.112	−0.773	24.851	−0.027	0.008	25.884***	517.508***
	INE nearby	6,075	0.001	0.128	−1.645	21.901	−0.019	0.018	11.637	272.090***
INE day-time trading	WTI nearby	2,520	−0.000	0.058	−0.278	17.961	−0.014	0.036	15.086	349.146***
	Brent nearby	2,520	0.000	0.062	0.521	12.970	−0.071	0.019	37.722***	740.317***
	INE nearby	2,520	0.001	0.105	−0.733	17.840	−0.020	−0.031	24.638***	234.678***
INE over-night trading	WTI nearby	3,556	0.003	0.143	−0.684	15.208	−0.019	0.009	18.893**	180.298***
	Brent nearby	3,556	0.003	0.137	−0.784	17.982	−0.025	0.014	17.792	265.852***
	INE nearby	3,556	0.001	0.142	−1.123	20.596	−0.013	0.034	10.147	129.813***
Panel B: Returns of Oman oil futures										
Sample	Nobs	Mean	SD	Skew	Excess Kurt	Lag1	Lag10	LB Q(10) for return	LB Q(10) for squared return	
Whole Sample	3,744	0.002	0.151	−5.580	153.695	−0.058	−0.046	0.013	40.940***	
INE daytime trading	614	0.005	0.096	3.269	42.008	−0.142	0.007	0.020	15.824***	
INE overnight trading	3,130	0.001	0.160	−5.792	146.328	−0.051	−0.050	0.019	33.576***	
Panel C: Correlations across WTI, Brent, INE, and Oman oil futures returns										
	Whole Sample			INE daytime trading			INE overnight trading			
	WTI	Brent	INE	WTI	Brent	INE	WTI	Brent	INE	
Brent	0.859			0.836			0.860			
INE	0.780	0.788		0.664	0.637		0.793	0.802		
Oman	−0.002	−0.007	0.048	0.021	0.032	0.022	−0.003	−0.009	0.050	
Panel D: Summary statistics of trading activity										
	WTI		Brent		INE		Oman			
	Mean	SD	Mean	SD	Mean	SD	Mean	SD	Mean	SD
Trading volume										
Nearby	622,613	252,473	281,995	102,500	148,339	79,967	2,913	1,089		
Second nearby	285,892	177,476	235,495	81,773	66	101	114	83		
Third nearby	103,441	35,435	105,715	31,188	11	26	69	73		
Open interest										
Nearby	368,143	167,376	391,656	166,000	23,301	10,011	11,987	8,122		
Second nearby	356,420	100,587	456,648	89,202	432	243	33	69		
Third nearby	203,252	36,709	234,720	59,212	64	24	19	38		

*Note:* Summary statistics for returns of WTI, Brent, INE, and Oman 5-min futures as well as trading activity from March 26 to June 26, 2018 are shown. From Bloomberg, WTI, Brent, INE, and Oman denote the log differences of 5-min trading prices of the corresponding nearby futures contracts. All measures are in percentage. LB Q(10) statistics with \*\* and \*\*\* denotes significance at 5% and 1%, respectively.

Abbreviations: INE, International Energy Exchange; LB Q(10), Ljung-Box's Q(10); Nobs, numbers of 5-min observations; WTI, West Texas Intermediate.



Panel D of Table 1 reports summary statistics of the major crude oil futures trading activity. China's oil futures have ranked the third largest crude oil futures market in terms of trading volumes, only after the WTI and Brent. For all crude oil futures, the trading volumes for the first nearby contracts are greater than the second, which in turn are greater than the third, implying that the nearby futures contracts are the most liquid and the most actively traded. In contrast to WTI and Brent futures counterparts, the trading volume of INE oil futures concentrates on the first nearby contract, which on average accounts for 99.9% of total futures trading. Meanwhile, INE oil futures have much smaller open interest than WTI and Brent counterparts. For example, the open interest of the nearby INE contract on average accounts for 15.7% of the corresponding future trading volume, suggesting that trading volume is mainly driven by speculative trading. Similar to trading volume, open interest of INE futures also concentrates on the first nearby contract, which on average accounts for 99.7% of total open interest. Compared with China's and two other crude oil futures, the trading of Oman futures is very thin while its open interest accounts for a higher percentage of the INE counterpart.

The Johansen's (1991) procedure is then applied to test for cointegration among the series of WTI, Brent, and INE as well as Oman futures prices.<sup>6</sup> Specifically, the optimal lags for level VAR are selected based on the Akaike Information Criterion (AIC), and the Johansen's trace and  $\lambda_{\max}$  tests are conducted for cointegration. To deal with the problem with or without a time trend, a sequential hypothesis testing procedure proposed by Johansen (1992) is followed. If there is a linear trend in the model, the hypothesis is labeled  $H_0(r)$ , which is an unrestricted case. If there is no linear trend in the model, the hypothesis is labeled  $H_0(r)^*$ , which is restricted. According to the sequential hypothesis testing procedure, hypotheses are tested in the following order:  $H_0(0)^*$ ,  $H_0(0)$ ,  $H_1(1)^*$ ,  $H_1(1)$ ,  $H_1(p)^*$ , and  $H_1(p)$ . When the null hypothesis first fails to be rejected in the sequence, testing is stopped, and the associated null hypothesis is accepted. Extending previous studies (e.g., Liu et al., 2015), the test statistics summarized in Table 2 indicate the existence of one cointegrating vector among WTI, Brent, and INE oil futures prices, among WTI, Brent, and Oman futures prices, as well as among Brent, INE, and Oman futures prices. The unreported result also shows that none of these markets are excluded in each of the cointegration vectors identified above, confirming that a long run relationship indeed connects all oil futures markets under consideration to some extent.

### 3 | ECONOMETRIC METHODOLOGY

Given the cointegration relationship, the empirical methodology we use is Vector Error Correction Model (VECM), with two different specifications of multivariate generalized autoregressive conditional heteroscedasticity (MGARCH) model. One of the MGARCH models is AG-DCC-GJR-GARCH model (Cappiello et al., 2006; Glosten, Jagannathan, & Runkle, 1993), which is flexible to investigate the presence of asymmetric responses in conditional variances and conditional correlations to negative returns. The other is the BEKK model (Engle & Kroner, 1995), which is flexible to account for both own- and cross-volatility spillovers, as well as volatility persistence.

#### 3.1 | VECM-AG-DCC-GJR-GARCH model

In this section, we present a multivariate VECM-AG-DCC-GJR-GARCH (1,1) model for 5-min returns of WTI, Brent, and INE nearby futures. The model jointly estimates asymmetric volatilities and asymmetric correlations, which may improve the specification substantially. Compared with a large body of the literature on asymmetric volatility, asymmetric correlation has received relatively less attention in the literature, which would be the focus of this study. We will derive continuous time series of time-varying conditional correlations through the AG-DCC-GJR-GARCH model to see how China's oil futures market is integrated with the global oil markets.

Since the crude oil futures price series are cointegrated, we consider the following vector error correction model after the preliminary search on the lag length:

<sup>6</sup>As only daily data are publicly available for crude oil cash markets, and the data only had 3-month history when we started the project, we would leave for future research the investigation of the price discovery function of China's crude oil futures market based on the cash-futures price relationship. As first pointed out in Yang and Leatham (1999), while it generally does not receive adequate attention in the literature on futures markets, the price discovery process also exists across multiple futures markets when they exist for a homogeneous or closely linked commodity. Noteworthy, such an argument on price discovery is also well received elsewhere, including those studies on price discovery performance of cross-listed stocks (e.g., Eun & Sabherwal, 2003).

TABLE 2 Cointegration tests

Panel A: Johansen cointegration test on WTI, Brent, and INE futures prices								
With linear trend					Without linear trend			
Trace test	C(5%)	$\lambda_{\text{Max}}$ test	C(5%)	$H_0$	Trace test	C(5%)	$\lambda_{\text{Max}}$ test	C(5%)
2.92	12.25	2.92	12.25	$r \leq 2$	2.48	9.24	2.48	9.24
11.59	25.32	8.67	18.96	$r \leq 1$	6.1	19.96	3.63	15.67
57.56**	42.44	45.97**	25.54	$r = 0$	50.47**	34.91	44.37**	22
Panel B: Johansen cointegration test on WTI, Brent, and Oman futures prices								
With linear trend					Without linear trend			
Trace test	C(5%)	$\lambda_{\text{Max}}$ test	C(5%)	$H_0$	Trace test	C(5%)	$\lambda_{\text{Max}}$ test	C(5%)
2.19	12.25	2.19	12.25	$r \leq 2$	2.79	9.24	2.79	9.24
9.00	25.32	6.81	18.96	$r \leq 1$	9.6	19.96	6.81	15.67
55.65**	42.44	46.66**	25.54	$r = 0$	56.31**	34.91	46.71**	22
Panel C: Johansen cointegration test on Brent, INE, and Oman futures prices								
With linear trend					Without linear trend			
Trace test	C(5%)	$\lambda_{\text{Max}}$ test	C(5%)	$H_0$	Trace test	C(5%)	$\lambda_{\text{Max}}$ test	C(5%)
2.61	12.25	2.61	12.25	$r \leq 2$	2.02	9.24	2.02	9.24
10.96	25.32	8.35	18.96	$r \leq 1$	5.71	19.96	3.69	15.67
92.29**	42.44	81.33**	25.54	$r = 0$	69.33**	34.91	63.62**	22

Note: The table reports Johansen's cointegration tests for WTI, Brent, and INE as well as Oman futures prices from March 26 to June 26, 2018.  $r$  is the number of cointegrating vectors.  $C$  is the trace test critical values. When test statistics are greater than  $C(5\%)$ , we reject the null hypothesis that the number of cointegrating vectors is less than or equal to  $r$ . \*\*denotes significance at 5%.

$$\Delta X_t = \alpha \beta' X_{t-1} + \sum_{i=1}^{k-1} \Gamma_i \Delta X_{t-i} + \mu + e_t \quad e_t \sim N(0, H_t), \quad (1)$$

where  $X_t$  is a  $n \times 1$  vector of futures prices in natural logarithm,  $\beta' X_t$  is the one period lagged deviation from the long-run equilibrium relationship, and the  $n \times 1$  vector,  $\alpha$ , measures the response of the endogenous variables to deviations from the long-run equilibrium relationship. The rank of  $\Pi = \alpha \beta'$  determines the number of cointegration vectors or the cointegration rank.  $e_t$  is a  $n \times 1$  vector of innovations, and  $H_t$  is the conditional variance-covariance matrix of  $r_t$  (or equivalently  $e_t$ ).

$H_t$  can be further decomposed into the diagonal matrix conditional standard deviation,  $D_t$ , and the conditional correlation matrix  $R_t$ :

$$H_t = D_t R_t D_t, \quad (2)$$

where

$$\begin{aligned} D_t &= \text{diag}(h_{it}^{1/2}), \\ h_{it} &= \omega_i + \alpha_i \varepsilon_{i,t-1}^2 + \beta_i h_{i,t-1} + \gamma_i \{\min(\varepsilon_{i,t-1}, 0)\}^2, \\ \varepsilon_t &= D_t^{-1} r_t \sim N(0, 1), \\ R_t &= (\rho_{ij,t}) = E_{t-1}(\varepsilon_{i,t} \varepsilon_{j,t}). \end{aligned} \quad (3)$$

Note that in this model the conditional volatility  $h_{it}$  is assumed to follow a univariate asymmetric GARCH (1,1) process as in Glosten et al. (1993). The conditional correlation estimator is

$$\rho_{ij,t} = q_{ij,t} / \sqrt{q_{ii,t} q_{jj,t}}, \quad (4)$$

where  $q_{ij,t}$  is conditional covariance if  $i \neq j$  and conditional variance if  $i = j$ .

$R_t$  can be written in terms of covariance matrix  $Q_t = (q_{ij,t})$  as follows:

$$R_t = (\text{diag}(Q_t))^{-1/2} Q_t (\text{diag}(Q_t))^{-1/2}. \quad (5)$$

As in Cappiello et al. (2006), the evolution of  $Q_t$  is governed by the asymmetric generalized DCC process:

$$Q_t = \bar{R} + A \cdot (\varepsilon_{t-1} \varepsilon'_{t-1} - \bar{R}) + B \cdot (Q_{t-1} - \bar{R}) + G \cdot (\eta_{t-1} \varepsilon'_{t-1} \eta'_{t-1} - \bar{N}), \quad (6)$$

where  $\bar{R} = E[\varepsilon_t \varepsilon'_t]$ ,  $A$ ,  $B$ , and  $G$  are square  $(n \times n)$ , symmetric matrices,  $\cdot$  is a Hadamard product,  $\eta_t = \min(\varepsilon_t, 0)$ , and  $\bar{N} = E[\eta_t \eta'_t]$ .

We can choose a diagonal parameterization for  $A$ ,  $B$ , and  $G$  as follows

$$A = \alpha_C \alpha'_C, \quad B = \beta_C \beta'_C, \quad G = \gamma_C \gamma'_C, \quad (7)$$

where  $\alpha_C$ ,  $\beta_C$ , and  $\gamma_C$  are  $n \times 1$  vectors, so that for any  $W$

$$A \cdot W = \text{diag}\{\alpha_C\} W \text{diag}\{\alpha_C\}. \quad (8)$$

Hence, for any  $i$  and  $j$ , we obtain the following expression to be used in the subsequent empirical analysis:

$$q_{ij,t} = \bar{\rho}_{ij} + \alpha_{i,C} \alpha_{j,C} (\varepsilon_{i,t-1} \varepsilon_{j,t-1} - \bar{\rho}_{ij}) + \beta_{i,C} \beta_{j,C} (q_{ij,t-1} - \bar{\rho}_{ij}) + \gamma_{i,C} \gamma_{j,C} (\eta_{i,t-1} \eta_{j,t-1} - \bar{N}_{i,j}). \quad (9)$$

Assuming normality, the log-likelihood function of the sample is given by

$$\begin{aligned} L = \sum_{t=1}^T l_t &= -\frac{1}{2} \sum_t \left( \log(2\pi) + \log |D_t R_t D_t| + r'_t D_t^{-1} R_t^{-1} D_t^{-1} r_t \right) \\ &= -\frac{1}{2} \sum_t \left( \log(2\pi) + 2 \ln |D_t| + r'_t D_t^{-2} r_t - \varepsilon'_t \varepsilon_t + \ln |R_t| + \varepsilon'_t R_t^{-1} \varepsilon_t \right). \end{aligned} \quad (10)$$

Let the parameters in  $D$  be denoted  $\theta = (\mu_i, \lambda_{ij}, \omega_i, \alpha_i, \beta_i)$  and the additional parameters in  $R$  be denoted  $\phi = (\alpha_{i,C}, \beta_{i,C}, \gamma_{i,C})$ . The log likelihood function can be written as the sum of a volatility part and a correlation part:

$$L(\theta, \phi) = L_V(\theta) + L_C(\theta, \phi), \quad (11)$$

where the volatility term is apparently the sum of individual GARCH likelihoods

$$L_V(\theta) = -\frac{1}{2} \sum_t \left( \log(2\pi) + 2 \ln |D_t| + r'_t D_t^{-2} r_t \right) \quad (12)$$

and the correlation term is:

$$L_C(\theta, \phi) = -\frac{1}{2} \sum_t \left( -\varepsilon'_t \varepsilon_t + \ln |R_t| + \varepsilon'_t R_t^{-1} \varepsilon_t \right). \quad (13)$$

Hence, the two-step estimation approach can be followed, as proposed in Engle (2002) and Cappiello et al. (2006), to maximize the likelihood function, which is to find

$$\hat{\theta} = \arg \max \{L_V(\theta)\}, \quad (14)$$



and then take this value as given in the second stage,

$$\text{Max}_{\varphi} L_C \left( \hat{\theta}, \varphi \right). \quad (15)$$

In sum, there are two stage estimations of the conditional covariance matrix for the AG-DCC models. First, VAR(1) and univariate GARCH models are fit for each of these oil futures returns. Second, the estimated standard deviations of oil futures returns are used to estimate the parameters of the conditional correlations using the AG-DCC model. In the second-stage analysis, we estimate the DCC model as a benchmark and then extend it into the asymmetric DCC model assuming the different impact of a negative shock on all pairwise correlations. Having ensured the presence of asymmetric correlations, we further examine the more general AG-DCC model.

### 3.2 | VECM-GARCH-BEKK model

To take further account of volatility spillovers and see how information transmits from one market to another, crude oil futures can be jointly modeled in a VAR-GARCH model with BEKK specification. In particular, the information transmission through the volatility linkage is investigated by estimating the conditional variance-covariance matrix  $H_t$  in Equation (16),

$$H_t = CC' + A(\varepsilon_{t-1}\varepsilon'_{t-1})A' + BH_{t-1}B', \quad (16)$$

where  $C$  is an upper triangle matrix of constants  $c_{ij}$ ,  $A$  is a matrix of elements  $a_{ij}$  that captures direct spillover effect from market  $i$  to market  $j$ , and  $B$  is a matrix of elements  $b_{ij}$  that measure direct persistent effects in volatility transmissions between markets  $i$  and  $j$ .

In the case of three markets,  $H$ ,  $C$ ,  $A$ , and  $B$  can be written as follows:

$$H_t = \begin{pmatrix} h_{11} & h_{12} & h_{13} \\ h_{21} & h_{22} & h_{23} \\ h_{31} & h_{32} & h_{33} \end{pmatrix}, \quad C_t = \begin{pmatrix} c_{11} & c_{12} & c_{13} \\ 0 & c_{22} & c_{23} \\ 0 & 0 & c_{33} \end{pmatrix}, \quad A = \begin{pmatrix} a_{11} & a_{12} & a_{13} \\ a_{21} & a_{22} & a_{23} \\ a_{31} & a_{32} & a_{33} \end{pmatrix}, \quad B = \begin{pmatrix} b_{11} & b_{12} & b_{13} \\ b_{21} & b_{22} & b_{23} \\ b_{31} & b_{32} & b_{33} \end{pmatrix}. \quad (17)$$

Specifically, Equation (16) can be expanded using Equation (17) as follows:

$$\begin{aligned} H_t = & \begin{bmatrix} c_{11} & c_{12} & c_{13} \\ 0 & c_{22} & c_{23} \\ 0 & 0 & c_{33} \end{bmatrix} \begin{bmatrix} c_{11} & c_{12} & c_{13} \\ 0 & c_{22} & c_{23} \\ 0 & 0 & c_{33} \end{bmatrix} + \begin{bmatrix} a_{11} & a_{12} & a_{13} \\ a_{21} & a_{22} & a_{23} \\ a_{31} & a_{32} & a_{33} \end{bmatrix} \begin{bmatrix} \varepsilon_{1,t-1}^2 & \varepsilon_{1,t-1}\varepsilon_{2,t-1} & \varepsilon_{1,t-1}\varepsilon_{3,t-1} \\ \varepsilon_{2,t-1}\varepsilon_{1,t-1} & \varepsilon_{2,t-1}^2 & \varepsilon_{2,t-1}\varepsilon_{3,t-1} \\ \varepsilon_{3,t-1}\varepsilon_{1,t-1} & \varepsilon_{3,t-1}\varepsilon_{2,t-1} & \varepsilon_{3,t-1}^2 \end{bmatrix} \begin{bmatrix} a_{11} & a_{12} & a_{13} \\ a_{21} & a_{22} & a_{23} \\ a_{31} & a_{32} & a_{33} \end{bmatrix} \\ & + \begin{bmatrix} b_{11} & b_{12} & b_{13} \\ b_{21} & b_{22} & b_{23} \\ b_{31} & b_{32} & b_{33} \end{bmatrix} \begin{bmatrix} h_{11,t-1} & h_{12,t-1} & h_{13,t-1} \\ h_{21,t-1} & h_{22,t-1} & h_{23,t-1} \\ h_{31,t-1} & h_{32,t-1} & h_{33,t-1} \end{bmatrix} \begin{bmatrix} b_{11} & b_{12} & b_{13} \\ b_{21} & b_{22} & b_{23} \\ b_{31} & b_{32} & b_{33} \end{bmatrix}. \quad (18) \end{aligned}$$

With the above specification, we can use off-diagonal parameters in matrices  $A$  and  $B$  to explain the volatility spillover effect. For example, the off-diagonal parameter  $a_{ij}$  measures the transmission of the absolute size of the return shocks, as measured by squared values of lagged unpredictable returns, originating from market  $i$  in the previous period to the current period's conditional volatility in market  $j$ , while the dependence of the conditional volatility in market  $j$  on that of market  $i$  in the previous period is measured by the parameter  $b_{ij}$ .

Nevertheless, not all the channels of volatility spillovers can be exhaustively accounted for in the above specification, so such interpretation on the off-diagonal parameters, though perhaps revealing, should be considered preliminary. Unfortunately, the interpretation of other parameters from the GARCH-BEKK model is generally not straightforward. Following Fleming, Kirby, and Ostdiek (1998), we use the time-varying cross-market conditional correlation, computed as  $CC_{ij} = h_{ij,t}/(h_{ii,t}h_{jj,t})^{1/2}$ , to gauge the volatility linkage across the markets.

## 4 | EMPIRICAL RESULTS

This section presents the results of both VECM-AG-DCC-GJR-GARCH and VECM-GARCH-BEKK models. Since there are several thousands of observations for the samples under consideration, we consider the statistical significance of parameter estimates at the 5% level or lower as appropriate to make the inference in the analysis below.

### 4.1 | The error correction and asymmetric patterns

Table 3 shows the parameter estimates of the mean and volatility models for WTI, Brent, and INE oil futures.<sup>7</sup> In Panel A of VECM(1) results for the whole sample, WTI oil futures returns cannot be predicted by its own lag and other lagged oil futures returns. In contrast, the predictability of Brent and INE oil futures returns is stronger: Brent oil futures returns can be predicted by its own lag and lagged WTI futures returns while the lagged Brent futures returns is a strong predictor of INE returns. Moreover, the error correction term is significantly associated with China's oil futures returns but not with the two leading global oil futures returns. This suggests that China's futures market reacts to deviations from the long-run equilibrium among these three markets while the WTI and Brent futures do not, plausibly implying that China's crude oil futures market generates less long-run information than the two leading global crude oil futures during the sample period.

When we break the whole sample into INE daytime and overnight trading subsamples, the pattern during the INE overnight trading is similar to that of the whole sample. In particular, the association of the error correction term with China's oil futures is significant while it is not the case for the WTI and Brent futures markets. In contrast, during the INE daytime trading, the reaction of China's oil futures to deviations from the long-run equilibrium is not significant and at the 5% level. Moreover, the predictability of INE oil futures returns disappear during the INE daytime trading while the lag of INE futures is a strong predictor of future WTI and Brent returns. The results suggest that China's oil futures market has more informational advantage during the INE daytime trading than during the INE overnight trading.

The information production argument can offer a plausible explanation to the above interesting phenomenon. Using high frequency futures data, Andersen, Bollerslev, Diebold, and Vega (2007) detect strong but short-lived effects of macroeconomic news on stock, bond, and foreign exchange markets in an international context. The macroeconomic news of the two largest economies (i.e., the United States and China) obviously matter for the global crude oil market. Hence, we have a similar argument that China's oil futures returns can predict WTI and Brent futures returns due to more information production based on Chinese macroeconomic news releases in the INE daytime trading. In the INE overnight trading period, there is far more macroeconomic news regularly released in the United States and UK markets, which triggers the reaction of China's oil futures to deviations from the long-run equilibrium.

In addition to relatively scarce information in China versus the United States and the UK during the INE overnight session, the differential informational role of institutional trading versus individual trading can also play a role here. Zhao and Wan (2018) find that despite the fact that individual investors account for approximately 90% of the entire Chinese commodity futures market, only a certain type of institutional trading is associated with permanent price movements, while individual trading is always information-biased. Arguably, it is likely that informed institutional trading in China would take place during regular work hours that overlaps with the INE daytime trading rather than the INE overnight trading. Wellenreuther and Voelzke (2019) also point out extremely speculative trading behavior on Chinese commodity futures markets. This might also suggest higher trading shares of extremely speculative individual investors in China, implied by higher trading volume and yet lower informational content during the INE overnight trading. Future research may examine the conjecture with the trade-by-trade record with the proprietary information of institutional and individual accounts, or hedgers versus speculators.

As shown in Panel B of the results of the GJR GARCH model, most coefficients are positive and highly significant in the whole sample. The volatility for each asset return displays a highly persistent fashion since the sum of the estimated coefficients  $\alpha$  and  $\beta$  in each variance equation is close to unity for all of the cases. Moreover, all asset returns exhibit asymmetric volatilities, indicating that volatilities increase after negative shocks for each return. The asymmetry of INE volatility is greater than WTI and Brent counterparts since the magnitude of the estimated coefficient  $\gamma$  for INE is bigger

<sup>7</sup> Perhaps due to the complexity of the model we use and the dramatic increase in the number of parameters that need to be estimated when additional variables are added, conducting the analysis based on all four oil futures markets often presented estimation difficulty related to a lack of convergence.

**TABLE 3** Results of VECM-GJR-GARCH models for WTI-Brent-INE nearby futures

Panel A: estimation results of VECM(1) model												
Return <i>i</i>	Whole sample				INE daytime trading sample				INE overnight trading sample			
	Lagged	Lagged	Lagged	Lagged	Lagged	Lagged	Lagged	Lagged	Lagged	Lagged	Lagged	Lagged
	WTI	Brent	INE	ECT	WTI	Brent	INE	ECT	WTI	Brent	INE	ECT
WTInearby	−0.027	0.021	−0.008	0.042	−0.002	−0.082**	0.057***	0.044	−0.012	0.052	−0.062**	0.071
	(−1.069)	(0.822)	(−0.438)	(0.215)	(−0.065)	(−2.374)	(4.040)	(0.269)	(−0.362)	(1.483)	(−2.110)	(0.229)
Brentnearby	0.067***	−0.082***	−0.004	0.103	0.207***	−0.282***	0.050***	0.142	0.066**	−0.039	−0.054	0.113
	(2.717)	(−3.252)	(−0.258)	(0.545)	(5.216)	(−7.781)	(3.400)	(0.834)	(2.018)	(−1.170)	(−1.919)	(0.385)
INEnearby	0.018	0.088***	−0.088***	−0.707***	−0.038	0.064	−0.028	−0.535	0.041	0.121***	−0.136***	−0.704**
	(0.650)	(3.116)	(−4.465)	(−3.301)	(−0.573)	(1.056)	(−1.136)	(−1.870)	(1.202)	(3.481)	(−4.703)	(−2.321)
Panel B: estimation results of GJR-GARCH model												
Sample Return <i>i</i>	Whole sample			INE daytime trading sample			INE overnight trading sample					
	$\alpha_i$	$\beta_i$	$\gamma_i$	$\alpha_i$	$\beta_i$	$\gamma_i$	$\alpha_i$	$\beta_i$	$\gamma_i$			
WTInearby	0.265***	0.811***	0.089***	0.168	0.388	0.168	−0.003	0.865***	0.122***			
	(65.502)	(813.969)	(22.047)	(0.956)	(0.671)	(0.957)	(−0.137)	(13.113)	(5.153)			
Brentnearby	0.067***	0.846***	0.178***	0.074***	0.690***	0.101***	0.083***	0.878***	0.031			
	(24.260)	(893.468)	(64.764)	(5.005)	(17.122)	(6.859)	(3.491)	(18.543)	(1.272)			
INEnearby	0.152***	0.723***	0.166***	0.120***	0.042	0.220***	0.108***	0.824***	0.084***			
	(39.989)	(425.418)	(43.631)	(4.782)	(1.009)	(8.646)	(4.148)	(17.032)	(3.207)			

Note: The mean and volatility models are as follows:

$$\Delta X_t = \alpha\beta'X_{t-1} + \sum_{i=1}^{k-1}\Pi_i\Delta X_{t-i} + \mu + \varepsilon_t\varepsilon_t \sim N(0, H_t), H_t = D_tR_tD_t,$$

$$D_t = \text{diag}(h_{it}^{1/2}), h_{it} = \omega_i + \alpha_i\varepsilon_{i,t-1}^2 + \beta_i h_{i,t-1} + \gamma_i(\min(\varepsilon_{i,t-1}, 0))^2,$$

where subscripts  $i \in \{1, 2, 3\}$  with 1 for the return of WTI nearby futures, 2 for the return of Brent nearby futures, 3 for the return of INE nearby futures, respectively. The  $t$  statistics are reported in parenthesis below the coefficients with \*\* and \*\*\* denoting significance at 5% and 1%, respectively. The sample period is from March 26 to June 26, 2018.

than those for the other two crude oil futures. Based on the INE daytime trading sample, the volatility for WTI oil futures is neither persistent nor asymmetric since coefficients  $\beta$  and  $\gamma$  are not significantly different from zeros. By contrast, INE oil futures show an even stronger evidence of asymmetric volatilities but not persistent volatility during daytime trading. Such patterns reversed during the overnight trading.

The different pattern of volatility clustering and asymmetry for China's oil futures can be explained through previous literature. Anderson and Bollerslev (1997) interpret volatility clustering in high frequency returns as a mixture of numerous heterogeneous short-run information arrivals. Based on this perspective, a plausible explanation might be that China's oil futures returns exhibit volatility clustering during its nighttime due to heterogeneous information arrivals, when the global crude oil markets (especially WTI) are trading in their daytime trading period with regular and ample information release. In contrast, there is no evidence for volatility clustering when China's oil futures market open in the INE daytime trading period, because much less information is released.<sup>8</sup>

As for asymmetric volatility, two popular explanations exist: the leverage effect and volatility feedback effect (time-varying risk premiums; see, e.g., Avramov, Chordia, & Amit, 2006). The significance of asymmetric volatility on WTI and Brent crude oil futures markets in this study is consistent with Kristoufek (2014), with additional new evidence of

<sup>8</sup>Also consistent with the information story, there is far more trading of INE futures during its nighttime trading when WTI and Brent futures are traded at their daytime.

significant asymmetric volatility on China's and Oman crude oil futures markets. The existence of stronger asymmetric volatility on China's crude oil futures market could simply reflect higher risk aversion to downside risk and thus stronger volatility feedback effect of Chinese investors on China's oil futures market in its infancy.<sup>9</sup> The phenomenon that asymmetric volatility is more significant during the INE daytime trading than that during the INE overnight trading can also be consistent with the above explanation. This might relate with the fact that a relatively higher percentage of traders on China's oil futures market during the INE daytime trading would be Chinese domestic investors, and thus, present an even stronger volatility feedback effect during the INE overnight trading.

Following Yang, Zhou, and Wang (2010), the time series profile of the three crude oil futures' conditional volatilities over the full period, daytime, and overnight trading subperiods is shown in Panel A of Table 5. The mean of these volatilities are close to their unconditional counterparts, which suggest the adequacy of conditional volatility modeling. Consistent with the use of GARCH models, the estimated volatilities were strongly serially correlated in both the full sample and the nighttime subperiod. By contrast, the serial correlations of estimated volatilities in the daytime sub-sample are significantly lower, especially for the INE oil futures.

Table 4 reports the estimation results of the AG-DCC model. The estimated log-likelihood values and the resulting likelihood ratio test statistics (not reported here) suggest that the AG-DCC model fits significantly better than the benchmark DCC model, underscoring the importance of more flexible modeling of conditional correlation dynamics. All asymmetry parameters are significantly positive, which suggests that the correlations of any two oil futures market returns tend to be higher responding to their negative returns. Such an asymmetric correlation pattern implies that negative shocks tend to make the three oil futures markets comove more strongly. Especially, as the INE market is (to a large extent) integrated with the two major global oil futures markets, a negative systematic shock could increase volatility and induce risk premium increases for all oil futures markets, causing a price drop in INE oil futures and the correlation increase between INE and the other two futures markets.

More evidence of asymmetric correlations is summarized in Matrix G, as shown in Panel D. Panels B and C also show that the shocks to correlations are typically persistent. To further explore asymmetry in correlation, we will study correlation dynamics and volatility spillovers in the following two sections.

## 4.2 | Correlation dynamics

We can obtain the conditional correlation time series based on Equations (5) and (6). Figure 2 plots the conditional correlations between the two global crude oil futures markets, WTI and Brent. Based on the full sample, the correlation between these two major oil futures returns swings from 22.8% to 96.9% with a mean of 85.1%. During the INE daytime trading period, the correlation is 84.9% on average between WTI and Brent oil futures markets, ranging from 56.4% to 89.5%. During the INE overnight trading period, the correlation between WTI and Brent is more volatile, ranging from 21.7% to 97.5%, and yet, it still has the same mean of 85.0% as in the full sample. Obviously, extending research by Liu et al. (2015), these two major international crude oil futures markets are, in general, highly integrated with each other, with occasional dramatic changes in the correlation even during the 3-month sample period.

It is more interesting to observe much interdependence between the nascent Shanghai INE crude oil futures market and the two major crude oil futures markets in the world. Figure 3 plots the estimated conditional correlations between the INE and WTI oil futures markets. Based on the full sample, the correlation swings from 22.4% to 95.9% with the mean of 77.3% between these two oil futures returns, suggesting a generally high degree of interdependence between China's and WTI futures markets and yet significant time-variation of such interdependence. Interestingly, during the INE daytime trading period, the correlation between the two markets has a lower mean of 67.2%, ranging from 38.5% to 79.7%. During the INE overnight trading period, the correlation between the two markets is from 27.2% to 95.8% with a higher mean of 78.8%. The different patterns of conditional correlations during INE daytime and overnight trading periods are also consistent with the previous information-based explanation. That is, China's crude oil futures are

<sup>9</sup>While it is not clear about how the leverage effect could explain the daily asymmetric volatility on crude oil futures markets, the trading-based explanation of Avramov et al. (2006) might also shed some light on the issue. In particular, their explanation points out that the existence of asymmetric volatility may be due to the non-informational herding trades which increase volatility following price declines. Given the higher percentage of individual investors and thus probably more herding trades on Chinese futures markets in general than major international crude oil markets, it can also explain the finding of stronger asymmetric volatility on China's crude oil futures market than on two major international crude oil markets. Nevertheless, it is harder to explain why asymmetric volatility is more significant during the INE daytime trading than during the INE overnight trading, unless there is additional evidence that compared with the INE overnight trading, a much higher percentage of Chinese investors during the INE daytime trading are institutional investors (presumably less vulnerable to herd trading), rather than individual investors. We leave more thorough investigation for future research.

**TABLE 4** Estimation results of the AG-DCC models for WTI-Brent-INE nearby futures

<b>Panel A: Parameters of the AG-DCC models</b>									
	<b>Whole sample</b>			<b>INE daytime trading sample</b>			<b>INE overnight trading sample</b>		
<i>i</i>	$\alpha_{i,C}$	$\beta_{i,C}$	$\gamma_{i,C}$	$\alpha_{i,C}$	$\beta_{i,C}$	$\gamma_{i,C}$	$\alpha_{i,C}$	$\beta_{i,C}$	$\gamma_{i,C}$
WTI nearby	0.175*** (27.942)	0.962*** (299.546)	0.237*** (15.587)	0.054*** (3.292)	0.974*** (99.248)	0.199*** (5.101)	0.192*** (18.947)	0.975*** (316.355)	0.136*** (7.150)
Brent nearby	0.079*** (15.559)	0.981*** (450.647)	0.204*** (15.812)	0.018 (1.219)	0.986*** (159.152)	0.111*** (4.445)	0.133*** (18.886)	0.984*** (793.755)	0.144*** (9.994)
INE nearby	0.105*** (13.509)	0.969*** (402.032)	0.236*** (16.186)	0.130*** (8.145)	0.981*** (171.506)	0.139*** (4.865)	0.163*** (14.466)	0.969*** (445.418)	0.193*** (11.318)
<b>Panel B: Matrix A</b>									
<b>Whole sample</b>			<b>INE daytime trading sample</b>			<b>INE overnight trading sample</b>			
0.031	0.014	0.019	0.003	0.001	0.007	0.037	0.025	0.031	
0.014	0.006	0.008	0.001	0.000	0.002	0.025	0.018	0.022	
0.018	0.008	0.011	0.007	0.002	0.017	0.031	0.022	0.026	
<b>Panel C: Matrix B</b>									
<b>Whole sample</b>			<b>INE daytime trading sample</b>			<b>INE overnight trading sample</b>			
0.925	0.944	0.932	0.948	0.960	0.955	0.950	0.959	0.944	
0.943	0.962	0.950	0.960	0.972	0.967	0.959	0.968	0.953	
0.932	0.950	0.938	0.955	0.967	0.962	0.944	0.953	0.938	
<b>Panel D: Matrix G</b>									
<b>Whole sample</b>			<b>INE day time sample</b>			<b>INE night time sample</b>			
0.056	0.048	0.056	0.040	0.022	0.028	0.018	0.020	0.026	
0.048	0.042	0.048	0.022	0.012	0.015	0.020	0.021	0.028	
0.056	0.048	0.056	0.028	0.015	0.019	0.026	0.028	0.037	

Note: The correlation estimator  $R_t$  can be written in terms of covariance matrix  $Q_t = (q_{ij,t})$  as  $R_t = (\text{diag}(Q_t))^{-1/2} Q_t (\text{diag}(Q_t))^{-1/2}$ . The evolution of  $Q_t$  is given by:  $Q_t = \bar{R} + A \cdot (\varepsilon_{t-1} \varepsilon'_{t-1} - \bar{R}) + B \cdot (Q_{t-1} - \bar{R}) + G \cdot (\eta_{t-1} \eta'_{t-1} - \bar{N})$ , where  $\bar{R} = E[\varepsilon_t \varepsilon'_t]$ ,  $A$ ,  $B$ , and  $G$  are square, symmetric matrices,  $\cdot$  is a Hadamard product,  $\eta_t = \min(\varepsilon_t, 0)$ , and  $\bar{N} = E[\eta_t \eta'_t]$ .

A diagonal parameterization is chosen for  $A$ ,  $B$ , and  $G$ :  $A = \alpha_C \alpha'_C$ ,  $B = \beta_C \beta'_C$ ,  $G = \eta_C \eta'_C$ , where  $\alpha_C$ ,  $\beta_C$ , and  $\eta_C$  are  $3 \times 1$  vectors, so that for any  $i$  and

$$j, q_{ij,t} = \bar{q}_{ij} + \alpha_{i,C} \alpha_{j,C} (\varepsilon_{i,t-1} \varepsilon_{j,t-1} - \bar{q}_{ij}) + \beta_{i,C} \beta_{j,C} (q_{ij,t-1} - \bar{q}_{ij}) + \gamma_{i,C} \gamma_{j,C} (\eta_{i,t-1} \eta_{j,t-1} - \bar{N}_{ij}).$$

In Panel A, the  $t$  statistics are reported in parenthesis below the coefficients. \*\* and \*\*\* denoting significance at 5% and 1%, respectively. The sample period is from March 26 to June 26, 2018.

Abbreviations: INE, International Energy Exchange; WTI, West Texas Intermediate.

traded more actively during the INE overnight session (e.g., through intermarket spreading) to incorporate the information relevant to the global oil market, when WTI futures are traded during its daytime trading session with regular and ample information release. Specifically, Miao, Ramchander, Wang, and Yang (2018) document that a set of rich information release, including the monthly U.S. macroeconomic announcements and weekly oil and related energy product inventory announcement exert significant impacts on the WTI oil futures and option markets, which obviously may well be transmitted to China's oil futures market.

The conditional correlations between the Brent and INE futures markets show similar patterns, as plotted in Figure 4. In the full period, these two crude oil futures returns exhibit significant time-varying correlations, swinging from 32.0% to 97.4%, with a high level of interdependence of 70.7% as the average correlation. The different dynamics of conditional correlations at different times of the day is even more striking between the INE and Brent markets. In the INE daytime trading session, the correlation has a much lower mean of 63.6% with a range from 33.3% to 77.5%. In

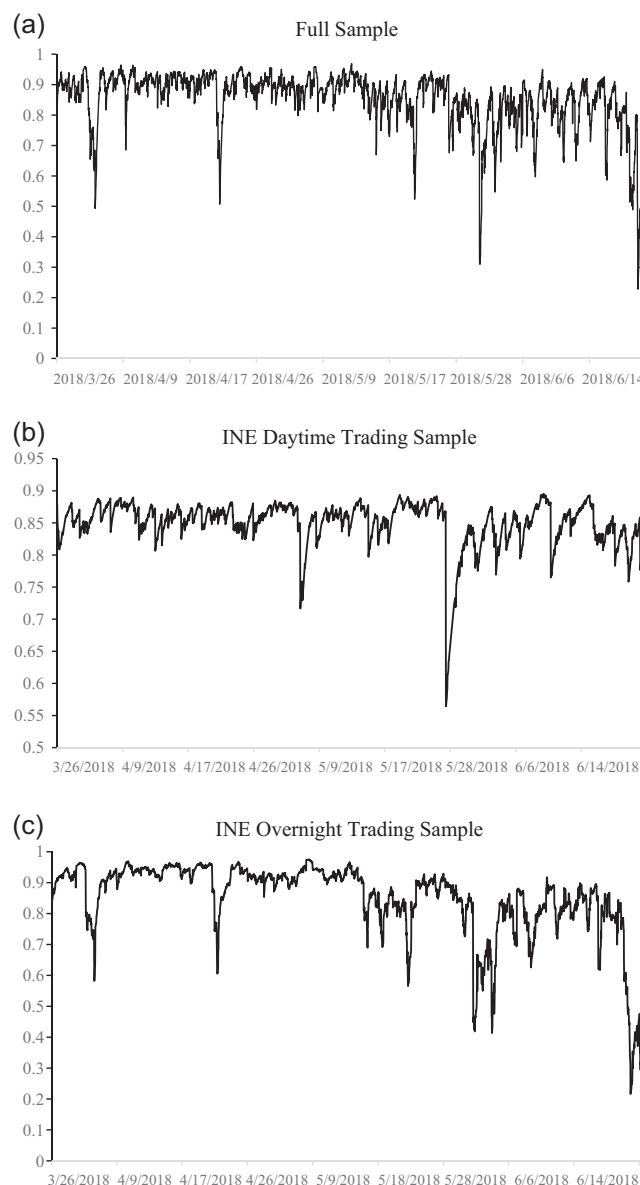


**FIGURE 2** Conditional correlation between WTI and Brent futures returns from VECM-GJR-GARCH-AG-DCC models. (a) Full sample; (b) INE daytime trading sample; (c) INE overnight trading sample. INE, International Energy Exchange; WTI, West Texas Intermediate

contrast, the correlations are much higher with a mean of 78.1% with a range from 34.1% to 98.3% during the INE overnight trading.

In sum, we have characterized the dynamics of pairwise correlations among WTI, Brent, and INE futures markets. To provide more information concisely about the correlation dynamics, the summary statistics for the derived conditional correlation series are presented in Panel B of Table 5. On average, three pairs of correlations are higher than 70%, except for the pairs of the INE and the other two crude oil futures during the daytime trading. Thus, China's crude oil futures are rather well integrated with the global crude oil futures markets, especially during its overnight trading session when much information from the daytime session of the WTI and Brent markets is available (e.g., Miao et al., 2018). We also compare the average of each conditional correlation series to its unconditional counterpart and find that they are generally close to each other, validating the adequacy of empirical models used here. Additional analyses are reported in Panel B. Autocorrelations and Ljung-Box Q tests show that all conditional correlations are highly persistent.



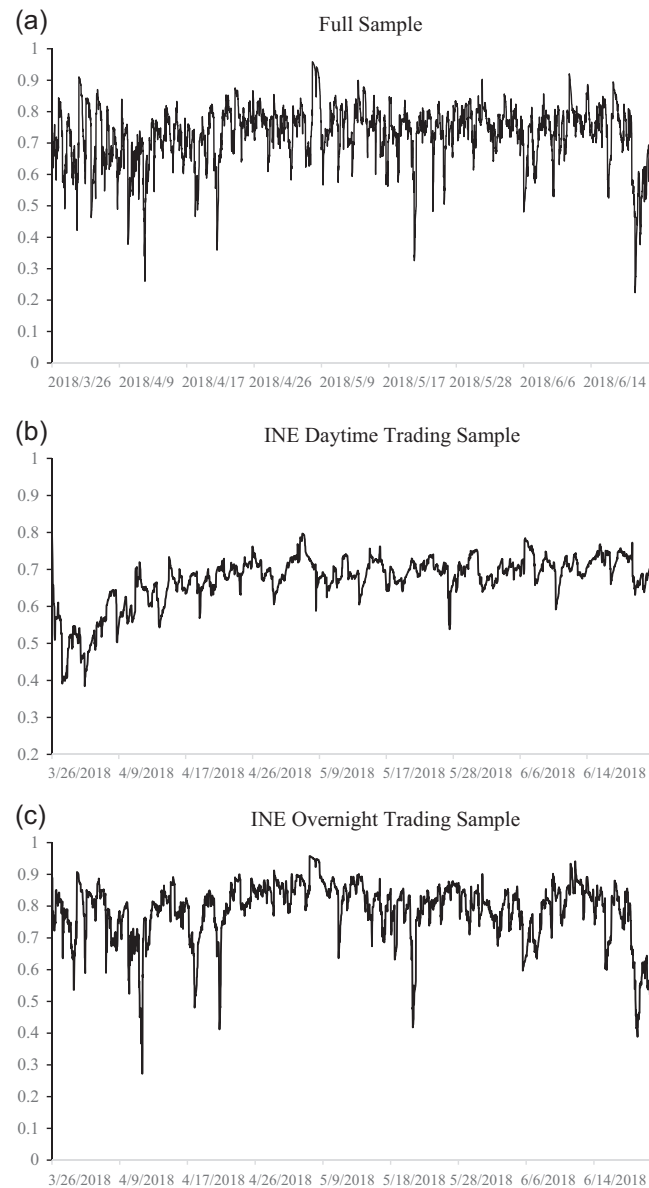


**FIGURE 3** Conditional correlation between WTI and INE futures returns from VECM-GJR-GARCH-AG-DCC models. (a) Full sample; (b) INE daytime trading sample; (c) INE overnight trading sample. INE, International Energy Exchange; WTI, West Texas Intermediate

### 4.3 | Volatility transmissions

Table 6 shows the estimation results of VECM-GARCH-BEKK models for WTI, Brent, and INE oil futures. The VECM (1) results shown in Panel A are similar to those in Panel A of Table 3. In the full sample and the INE overnight trading subsample, China's crude oil futures react to deviations from the long-run equilibrium while the WTI and Brent futures do not. However, this pattern is not significant in the INE daytime trading. Moreover, China's crude oil futures returns can predict the two global crude oil futures returns in its daytime trading, while such predictive power is much weakened during the INE overnight trading.

We focus on the pattern of information transmission through volatility by examining estimates of off-diagonal parameters in Panels B and C. In the entire sample, most off-diagonal parameters are statistically significant at least at 5% level. The significance of the parameters which measure the cross-market impact of returns shocks on the volatility,  $a_{12}$  and  $a_{21}$ , suggests that the conditional volatility in the Brent oil futures depends on return shocks from the WTI oil futures in the previous period and vice versa. Meanwhile, there is strong evidence in favor of two-way persistent volatility transmissions between these two global futures, as reflected in the significance of  $b_{12}$  and  $b_{21}$ .

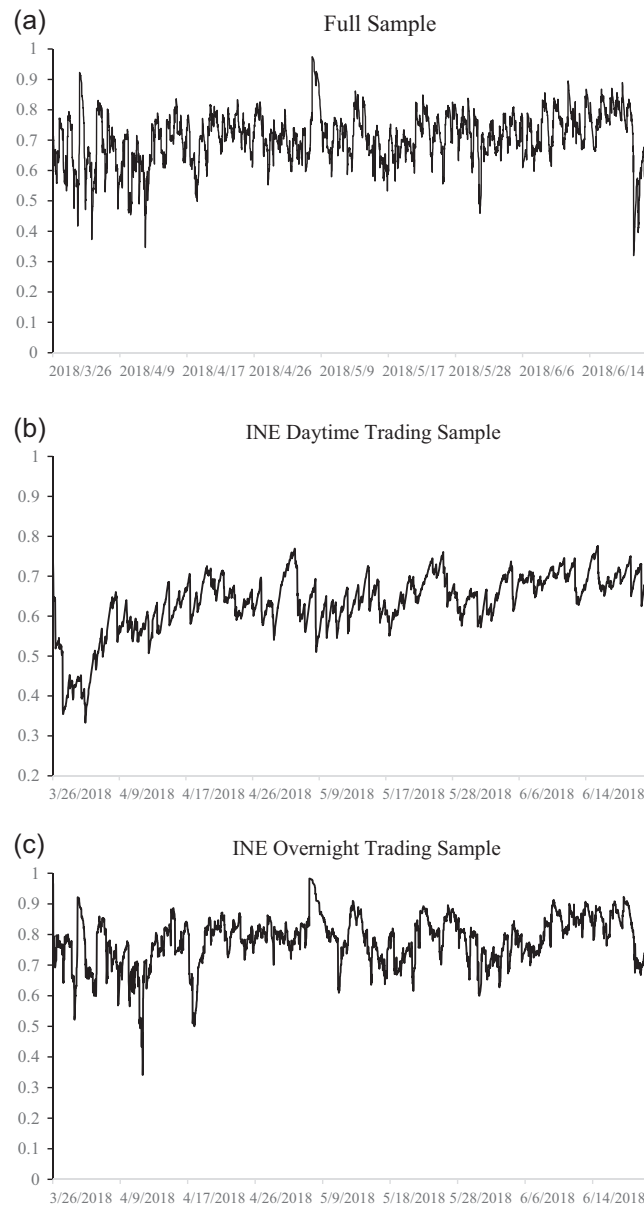


**FIGURE 4** Conditional correlation between Brent and INE futures returns from VECM-GJR-GARCH-AG-DCC models. (a) Full sample; (b) INE daytime trading sample; (c) INE overnight trading sample. INE, International Energy Exchange; WTI, West Texas Intermediate

More important,  $a_{13}$  and  $a_{23}$  are significant, suggesting one-way dependence of China's oil futures market volatility on past return shocks from the two global crude oil futures. Similarly, the conditional volatility in China's crude oil market depends on those of the WTI and Brent futures market in the previous period, as reflected in the significance of the parameters  $b_{13}$  and  $b_{23}$ . This evidence indicates substantial information spillover effects from the two global crude oil futures to China's crude oil market. In addition, there is two-way persistent volatility transmissions between WTI and INE oil futures since  $b_{31}$  is also significant.

When we break the sample into two sub-samples, there is further evidence for volatility (information) transmission across markets. In the INE daytime trading sample, there is two-way spillover effect between WTI and Brent as well as the spillover from the two global crude oil futures to China's crude oil futures, since  $a_{12}$  and  $a_{21}$  as well as  $a_{13}$  and  $a_{23}$  are all statistically significant at least at 5% level. In addition, as the significance of  $a_{32}$  shows, the return shocks originating from China's crude oil futures in the previous period transmit to the current period's conditional volatility in the Brent futures. Meanwhile, the parameters,  $b_{12}$ ,  $b_{21}$ , and  $b_{23}$  are statistically significant, in favor of two-way

**TABLE 5** Summary of volatilities and conditional correlations from GJR-GARCH-AG-DCC models

<b>Panel A: Conditional volatilities</b>								
	<b>Volatility</b>	<b>Nobs</b>	<b>Mean</b>	<b>Unconditional SD</b>	<b>Lag 1</b>	<b>Lag 5</b>	<b>Lag 10</b>	<b>LB Q(10)</b>
Full sample	WTI	6,071	0.114	0.116	0.908	0.564	0.403	24745.622***
	Brent	6,071	0.108	0.112	0.928	0.687	0.484	29352.429***
	INE	6,071	0.125	0.128	0.846	0.435	0.231	15015.717***
Day-Time sample	WTI	2,517	0.057	0.058	0.590	0.216	0.082	2128.374***
	Brent	2,517	0.058	0.062	0.851	0.521	0.269	7660.953***
	INE	2,517	0.101	0.105	0.175	0.028	0.005	99.335***
Night-Time sample	WTI	3,551	0.143	0.143	0.918	0.635	0.416	15176.218***
	Brent	3,551	0.134	0.137	0.930	0.685	0.484	17202.407***
	INE	3,551	0.139	0.142	0.902	0.590	0.367	13480.301***
<b>Panel B: Conditional correlations</b>								
	<b>Conditional Correlation</b>	<b>Nobs</b>	<b>Mean</b>	<b>Unconditional correlation</b>	<b>Lag 1</b>	<b>Lag 5</b>	<b>Lag 10</b>	<b>LB Q(10)</b>
Full sample	WTI-Brent	6,071	0.851	0.857	0.985	0.914	0.828	49819.048***
	WTI-INE	6,071	0.728	0.773	0.970	0.848	0.705	42798.837***
	Brent-INE	6,071	0.707	0.709	0.976	0.880	0.763	46093.602***
Day-time sample	WTI-Brent	2,517	0.849	0.836	0.967	0.849	0.728	17917.115***
	WTI-INE	2,517	0.672	0.597	0.986	0.931	0.871	21663.567***
	Brent-INE	2,517	0.636	0.559	0.988	0.937	0.876	21806.911***
Night time sample	WTI-Brent	3,551	0.850	0.846	0.992	0.955	0.906	31957.591***
	WTI-INE	3,551	0.788	0.790	0.976	0.872	0.749	26498.500***
	Brent-INE	3,551	0.781	0.781	0.976	0.885	0.774	27182.610***

*Note:* The table reports conditional volatilities and correlations for WTI, Brent, and INE 5-min y returns using the AG-DCC model. The estimates of conditional volatilities are derived from  $D_t$  as in Equations (2) and (3). The estimates of pairwise conditional correlations between asset returns  $i$  and  $j$  are derived as in Equations (6) and (7). The sample period is from March 26 to June 26, 2018.

Abbreviations: INE, International Energy Exchange; WTI, West Texas Intermediate.

persistent volatility transmissions between the two global futures as well as information spillover effect from the Brent futures to the INE futures.

In the INE overnight session sample, as the parameter  $a_{21}$  is statistically significant at least at the 5% level, the return shocks from the Brent futures in the previous period strongly impact the current conditional volatility in the WTI futures. Meanwhile, there is no strong evidence of persistent volatility transmissions among the three crude oil futures since all off-diagonal parameters in Panel C are not statistically significant at the 5% level.

To gauge the volatility linkage across the markets, we also calculate the conditional correlation between the three futures returns and report the mean statistic of estimated conditional correlation (not reported here). The results suggest an intensive volatility transmission between China's oil futures and other major futures markets, as shown by the high mean conditional correlations (71.5% between the WTI and INE markets and 70.7% between Brent and INE markets). In sum, our result here confirms strong bidirectional interactions in the intraday volatility between China's and global crude oil futures markets, implying that information in price innovations originated in either China's or the two major international oil futures markets is transmitted to the volatility of other markets.

#### 4.4 | Robustness checks

Note that the nearby INE futures contract in our sample expires in September 2018 while the WTI and Brent futures counterparts do not. To check the robustness of the main findings presented previously, we match the September 2018 futures contracts of WTI, Brent, and INE, and obtain 4,577 5-min observations, which are significantly fewer than the sample using nearby futures. Since there are much fewer observations of the September 2018 WTI and Brent futures

TABLE 6 Results of the VEM-GARCH-BEKK models for WTI-Brent-INE oil futures

Panel A: Estimation results of VECM (1) model												
Whole sample			INE daytime trading sample				INE overnight trading sample					
Return <i>i</i>	Lagged WTI	Lagged Brent	Lagged INE	Lagged ECT	Lagged WTI	Lagged Brent	Lag- ged INE	Lagged ECT	Lagged WTI	Lagged Brent	Lagged INE	Lagged ECT
WTI nearby	−0.026 (−1.006)	0.023 (0.877)	−0.011 (−0.625)	0.057 (0.290)	0.002 (0.040)	−0.080** (−2.323)	0.051*** (3.572)	0.068 (0.415)	−0.013 (−0.374)	0.053 (1.491)	0.062*** (−2.099)	0.088 (0.286)
Brent nearby	0.068*** (2.769)	−0.080*** (−3.200)	−0.007 (−0.424)	0.116 (0.610)	0.211*** (5.293)	−0.280*** (−7.739)	0.046*** (3.018)	0.163 (0.950)	0.065** (1.996)	−0.039 (−1.155)	−0.053* (−1.899)	0.144 (0.488)
INE nearby	0.019 (0.693)	0.090*** (3.153)	−0.091*** (−4.559)	−0.696*** (−3.243)	−0.035 (−0.527)	0.065 (1.078)	−0.032 (−1.275)	−0.516* (−1.799)	0.040 (1.194)	0.121*** (3.486)	−0.136*** (−4.695)	−0.693*** (−2.276)
Panel B: Estimation results of Matrix A in GARCH-BEKK model												
Whole sample			INE daytime trading sample				INE overnight trading sample					
Sample Return <i>i</i>	<i>a</i> <sub>11</sub>	<i>a</i> <sub>12</sub>	<i>a</i> <sub>13</sub>	<i>a</i> <sub>11</sub>	<i>a</i> <sub>12</sub>	<i>a</i> <sub>13</sub>	<i>a</i> <sub>11</sub>	<i>a</i> <sub>12</sub>	<i>a</i> <sub>11</sub>	<i>a</i> <sub>12</sub>	<i>a</i> <sub>13</sub>	
<i>a</i> <sub>1i</sub>	0.301*** (8.979)	0.626*** (20.350)	0.235*** (6.581)	0.022 (0.432)	−0.358*** (−7.619)	−0.369*** (−4.969)	0.359*** (8.840)	−0.010 (−0.249)	0.359*** (8.840)	−0.010 (−0.249)	−0.039 (−0.935)	
<i>a</i> <sub>2i</sub>	0.126*** (3.956)	−0.275*** (−8.881)	−0.173*** (−4.765)	0.387*** (8.002)	0.430*** (11.185)	0.386*** (4.517)	−0.092*** (−2.384)	0.269*** (7.919)	−0.092*** (−2.384)	0.269*** (7.919)	−0.056 (−1.529)	
<i>a</i> <sub>3i</sub>	−0.028 (−1.882)	0.004 (0.268)	0.471*** (19.194)	0.022 (0.867)	0.072*** (3.354)	0.394*** (9.061)	0.035 (1.062)	0.022 (0.696)	0.035 (1.062)	0.022 (0.696)	0.449*** (9.865)	
Panel C: estimation results of Matrix B in GARCH-BEKK model												
Whole sample			INE daytime trading sample				INE overnight trading sample					
Sample Return <i>i</i>	<i>b</i> <sub>11</sub>	<i>b</i> <sub>12</sub>	<i>b</i> <sub>13</sub>	<i>b</i> <sub>11</sub>	<i>b</i> <sub>12</sub>	<i>b</i> <sub>13</sub>	<i>b</i> <sub>11</sub>	<i>b</i> <sub>12</sub>	<i>b</i> <sub>11</sub>	<i>b</i> <sub>12</sub>	<i>b</i> <sub>13</sub>	
<i>b</i> <sub>1i</sub>	0.249*** (5.817)	1.066*** (26.312)	0.766*** (20.291)	−0.888*** (−11.594)	−1.048*** (−12.142)	−0.028 (−0.175)	−0.888*** (−46.372)	0.034 (1.960)	−0.888*** (−46.372)	0.034 (1.960)	0.000 (−0.012)	
<i>b</i> <sub>2i</sub>	0.785*** (16.560)	−0.228*** (−5.216)	0.360*** (8.461)	0.663*** (7.761)	1.273*** (28.864)	1.078*** (6.321)	0.041 (1.955)	−0.889*** (−51.757)	0.041 (1.955)	−0.889*** (−51.757)	0.004 (0.173)	
<i>b</i> <sub>3i</sub>	−0.091*** (−2.671)	−0.035 (−1.076)	−0.584*** (−12.454)	0.052 (1.645)	0.054 (1.006)	−0.808*** (−12.122)	−0.018 (−0.821)	−0.030 (−1.515)	−0.018 (−0.821)	−0.030 (−1.515)	−0.846*** (−27.795)	

Note: The mean and volatility models are as follows:

$$\Delta X_t = \alpha\beta'X_{t-1} + \sum_{i=1}^{k-1}\Gamma_i\Delta X_{t-i} + \mu + \varepsilon_t, \varepsilon_t \sim N(0, H_t), H_t = CC' + A(\varepsilon_{t-1}\varepsilon_{t-1}')A' + BH_{t-1}B'$$

where subscripts  $i \in \{1, 2, 3\}$  with 1 for the return of WTI nearby futures, 2 for the return of Brent nearby futures, 3 for the return of INE nearby futures, respectively. The  $t$  statistics are reported in parenthesis below the coefficients with \*\* and \*\*\* denoting significance at 5% and 1%, respectively. The sample period is from March 26 to June 26, 2018.

Abbreviations: INE, International Energy Exchange; WTI, West Texas Intermediate.

returns during the INE daytime trading period, we only examine the full sample period. The results of VECM-GJR-GARCH-AG-DCC model (available on request) confirm evidence for asymmetric volatilities and asymmetric correlations across these oil futures markets. The results of the VECM-GARCH-BEKK model (available on request) confirm that there is two-way volatility transmission between China's and major international oil futures markets.

We further take Oman oil futures into consideration since it closely resembles China's crude oil futures, reflecting medium and heavy sour conditions in Asia. As mentioned, Brent is relatively denser and has a higher sulfur content than WTI, and thus, it is more relevant and comparable to INE and Oman futures contracts. Hence, we include Brent in the analysis together with INE and Oman futures. Since there are very few observations of Oman futures returns during the INE daytime trading period, we only examine the full sample.

Panel A of Table 7 shows the parameter estimates of the VECM-GJR-GARCH-AG-DCC model for Brent, INE, and Oman oil futures. Interestingly, the results on mean equations show that Oman oil futures returns are affected by both INE and Brent returns of the previous period. Stronger predictability of Oman oil future implies weaker price discovery performance in the Oman market. Consistent with the above finding, the error correction term for the Oman futures market is also significant at the 5% level while it is not the case for the WTI and Brent futures returns. The results on variance equations show that Oman futures returns exhibited a higher degree of asymmetric volatility because its magnitude of the coefficient  $\gamma$  is greater than INE and Brent counterparts. Furthermore, the estimated coefficient  $\gamma_{i,c}$

**TABLE 7** Results of Brent-INE-Oman oil futures

<b>Panel A: Results of GJR-GARCH-AG-DCC model for Brent-INE-Oman oil futures</b>										
	Lagged Brent	Lagged INE	Lagged Oman	Lagged ECT	$\alpha_i$	$\beta_i$	$\gamma_i$	$\alpha_{i,c}$	$\beta_{i,c}$	$\gamma_{i,c}$
Brentnearby	−0.004 (−0.318)	−0.018 (−1.272)	−0.025** (−2.325)	0.001 (0.016)	0.156*** (114.514)	0.741*** (707.861)	−0.072*** (−53.223)	0.122*** (21.219)	0.793*** (210.401)	0.675*** (81.905)
INEnearby	0.019* (1.959)	−0.022* (−1.908)	−0.012 (−1.281)	−0.019 (−0.497)	0.043*** (33.441)	0.856*** (519.037)	0.076*** (59.557)	−0.553*** (−64.828)	0.552*** (35.518)	0.691*** (42.832)
Omannearby	0.315*** (41.394)	0.605*** (66.496)	−0.074*** (−10.416)	0.073** (2.439)	0.309*** (185.712)	0.781*** (140.438)	0.333*** (200.282)	0.002*** (6.592)	0.946*** (175.542)	0.261*** (49.413)
<b>Panel B: Results of the VAR-GARCH-BEKK models for Brent-INE-Oman oil futures</b>										
	Lagged Brent	Lagged INE	Lagged Oman	Lagged ECT	$a_{i1}$	$a_{i2}$	$a_{i3}$	$b_{i1}$	$b_{i2}$	$b_{i3}$
Brentnearby	−0.004 (−0.315)	−0.017 (−1.269)	−0.025** (−2.324)	0.000 (0.003)	0.668*** (24.477)	−0.038 (−1.174)	−0.128*** (−7.407)	0.704*** (48.874)	0.425*** (20.955)	0.100*** (11.092)
INEnearby	0.019** (1.965)	−0.022* (−1.902)	−0.012 (−1.280)	−0.020 (−0.526)	0.118*** (3.735)	−0.195*** (−6.144)	0.226*** (14.120)	−0.003 (−0.120)	0.082*** (3.468)	0.137*** (11.098)
Omannearby	0.315*** (41.390)	0.605*** (66.490)	−0.074*** (−10.416)	0.073** (2.445)	0.569*** (11.726)	−0.832*** (−21.322)	0.409*** (21.741)	−0.538*** (−37.708)	−0.320*** (−12.383)	0.842*** (125.765)

Note: This table presents the estimation results of two models for Brent, INE, and OMAN oil futures. In Panel A, the mean and volatility models are as follows:

$$\Delta X_t = \alpha \beta' X_{t-1} + \sum_{i=1}^{k-1} \Gamma_i \Delta X_{t-i} + \mu + \varepsilon_t, \varepsilon_t \sim N(0, H_t), H_t = D_t R_t D_t,$$

$$D_t = \text{diag}(h_{it}^{1/2}), h_{it} = \omega_i + \alpha_i \varepsilon_{i,t-1}^2 + \beta_i h_{i,t-1} + \gamma_i \{\min(\varepsilon_{i,t-1}, 0)\}^2,$$

The correlation estimator  $R_t$  can be written in terms of covariance matrix  $Q_t = (q_{ij,t})$  as  $R_t = (\text{diag}(Q_t))^{-1/2} Q_t (\text{diag}(Q_t))^{-1/2}$ . The evolution of  $Q_t$  is given by:

$$q_{ij,t} = \bar{\rho}_{ij} + \alpha_{i,c} \alpha_{j,c} (\varepsilon_{i,t-1} \varepsilon_{j,t-1} - \bar{\rho}_{ij}) + \beta_{i,c} \beta_{j,c} (q_{ij,t-1} - \bar{\rho}_{ij}) + \gamma_{i,c} \gamma_{j,c} (\eta_{i,t-1} \eta_{j,t-1} - \bar{N}_{ij})$$

In Panel B, the mean and volatility models are as follows:

$$\Delta X_t = \alpha \beta' X_{t-1} + \sum_{i=1}^{k-1} \Gamma_i \Delta X_{t-i} + \mu + \varepsilon_t, \varepsilon_t \sim N(0, H_t), H_t = CC' + A(\varepsilon_{t-1} \varepsilon_{t-1}')A' + BH_{t-1}B'$$

where subscripts  $i \in \{1, 2, 3\}$  with 1 for the return of Brent nearby futures, 2 for the return of INE nearby futures, 3 for the return of Oman futures, respectively. The  $t$  statistics are reported in parenthesis below the coefficients with \*\* and \*\*\* denoting significance at 5% and 1%, respectively. The sample period is from March 26 to June 26, 2018.

Abbreviations: INE, International Energy Exchange; WTI, West Texas Intermediate.

for Oman return is significantly smaller. From the AG-DCC model, the average conditional correlation between Brent and Oman returns is only 11.6%—much lower than the counterpart of 55.4% between Brent and INE returns. Overall, it suggests that China's crude oil futures market is better integrated with Brent futures markets than the Oman futures market is.

Panel B of Table 7 presents the estimation results of the VECM-GARCH-BEKK model for Brent, INE, and Oman oil futures. The results confirm stronger predictability of Oman oil future and significant reaction of Oman futures to deviations from the long-run equilibrium. Focusing on information transmission through volatility, we note that the estimates of off-diagonal parameters  $a_{ij}$ —which measure the transmission of the return shocks—are all statistically significant at least at a 5% level. It suggests that the conditional volatility in each oil futures depends on return shocks from the other two oil futures in the previous period. Meanwhile, most off-diagonal parameters  $b_{ij}$ —which measure the transmission of the pervious volatility—are statistically significant. In other words, there is strong bidirectional spillover effect in the intraday volatility among the three oil futures. From the BEKK model, the average conditional correlation between Brent and Oman returns is 13.2%, much lower than the counterpart of 56.6% between Brent and INE returns, and consistent with the result based on AG-DCC model. It suggests that the volatility linkage between INE and Brent crude oil futures markets is stronger than the case of the Oman oil futures market.

Table 8 repeats the analysis for WTI, Brent, and Oman oil futures. In both Panels A and B, Oman oil futures have stronger predictability and significantly react to deviations from the long-run equilibrium while WTI and Brent futures do not. For the

**TABLE 8** Results of WTI-Brent-Oman oil futures

Panel A: Results of GJR-GARCH-AG-DCC model for WTI-Brent-Oman oil futures										
	Lagged WTI	Lagged Brent	Lagged Oman	Lagged ECT	$\alpha_i$	$\beta_i$	$\gamma_i$	$\alpha_{i,C}$	$\beta_{i,C}$	$\gamma_{i,C}$
WTInearby	−0.034 (−1.683)	0.036 (1.775)	−0.007 (−0.792)	0.238 (1.225)	0.148*** (15.156)	0.873*** (68.943)	0.018** (2.358)	0.182*** (23.053)	0.969*** (337.335)	0.221*** (14.832)
Brentnearby	0.027 (1.320)	−0.036 (−1.773)	−0.023*** (−2.757)	0.247 (1.264)	0.126*** (28.040)	0.884*** (88.960)	0.012** (2.192)	0.101*** (16.113)	0.979*** (428.442)	0.229*** (14.980)
Omannearby	0.038** (2.476)	0.908*** (58.592)	−0.053*** (−8.205)	−0.542*** (−3.604)	0.083 (1.891)	0.570*** (41.580)	1.794*** (41.710)	0.010 (0.820)	−0.172 (−0.353)	−0.032 (−0.584)
Panel B: Results of the VAR-GARCH-BEKK models for WTI-Brent-Oman oil futures										
	Lagged WTI	Lagged Brent	Lagged Oman	Lagged ECT	$a_{i1}$	$a_{i2}$	$a_{i3}$	$b_{i1}$	$b_{i2}$	$b_{i3}$
WTInearby	−0.034 (−1.687)	0.036 (1.782)	−0.007 (−0.792)	0.239 (1.230)	0.226*** (6.302)	−0.048 (−1.254)	0.091*** (6.228)	0.535*** (9.793)	−0.427*** (−7.662)	0.141*** (5.055)
Brentnearby	0.026 (1.312)	−0.035 (−1.762)	−0.023*** (−2.756)	0.249 (1.272)	−0.288*** (−6.962)	0.030 (0.667)	0.003 (0.193)	−0.295*** (−5.434)	0.635*** (11.556)	0.181*** (6.686)
Omannearby	0.038** (2.476)	0.908*** (58.582)	−0.053*** (8.204)	−0.542*** (−3.604)	−0.044 (−1.516)	−0.045 (−1.479)	1.351*** (52.929)	0.078*** (5.475)	0.074*** (4.711)	0.361*** (21.889)

Note: This table presents the estimation results of two models for WTI, Brent, and Oman oil futures. In Panel A, the mean and volatility models are as follows:

$$\Delta X_t = \alpha\beta'X_{t-1} + \sum_{i=1}^{k-1}\Gamma_i\Delta X_{t-i} + \mu + \varepsilon_t \quad \varepsilon_t \sim N(0, H_t), \quad H_t = D_t R_t D_t,$$

$$D_t = \text{diag}(h_{it}^{1/2}), \quad h_{it} = \omega_i + \alpha_i \varepsilon_{i,t-1}^2 + \beta_i h_{i,t-1} + \gamma_i \{\min(\varepsilon_{i,t-1}, 0)\}^2,$$

The correlation estimator  $R_t$  can be written in terms of covariance matrix  $Q_t = (q_{ij,t})$  as  $R_t = (\text{diag}(Q_t))^{-1/2} Q_t (\text{diag}(Q_t))^{-1/2}$ . The evolution of  $Q_t$  is given by:

$$q_{ij,t} = \bar{\rho}_{ij} + \alpha_{i,C}\alpha_{j,C}(\varepsilon_{i,t-1}\varepsilon_{j,t-1} - \bar{\rho}_{ij}) + \beta_{i,C}\beta_{j,C}(q_{ij,t-1} - \bar{\rho}_{ij}) + \gamma_{i,C}\gamma_{j,C}(\eta_{i,t-1}\eta_{j,t-1} - \bar{N}_{i,j})$$

In Panel B, the mean and volatility models are as follows:

$$\Delta X_t = \alpha\beta'X_{t-1} + \sum_{i=1}^{k-1}\Gamma_i\Delta X_{t-i} + \mu + \varepsilon_t \quad \varepsilon_t \sim N(0, H_t), \quad H_t = CC' + A(\varepsilon_{t-1}\varepsilon'_{t-1})A' + BH_{t-1}B'$$

where subscripts  $i \in \{1, 2, 3\}$  with 1 for the return of WTI nearby futures, 2 for the return of Brent nearby futures, 3 for the return of Oman futures, respectively. The  $t$  statistics are reported in parenthesis below the coefficients with \*\* and \*\*\* denoting significance at 5% and 1%, respectively. The sample period is from March 26 to June 26, 2018.

Abbreviations: INE, International Energy Exchange; WTI, West Texas Intermediate.



**TABLE 9** Results of VECM-GJR-GARCH-AG-DCC Models for extended samples

<b>Panel A: Results for WTI-Brent-INE oil futures</b>										
	Lagged WTI	Lagged Brent	Lagged INE	Lagged ECT	$\alpha_i$	$\beta_i$	$\gamma_i$	$\alpha_{i,C}$	$\beta_{i,C}$	$\gamma_{i,C}$
WTInearby	−0.069** (−2.006)	0.123*** (3.359)	−0.039 (−1.884)	0.078 (0.433)	0.120*** (10.239)	0.770*** (129.115)	0.275*** (23.650)	0.204*** (13.888)	0.898*** (80.175)	0.357*** (17.051)
Brentnearby	0.029 (0.888)	0.033 (0.947)	−0.043** (−2.138)	−0.098 (−0.567)	0.088*** (4.155)	0.773*** (25.461)	0.223*** (10.726)	0.049*** (3.606)	0.890*** (83.558)	0.425*** (18.114)
INEnearby	−0.024 (−0.647)	0.062 (1.601)	0.030 (1.370)	−0.441** (−2.303)	0.095*** (8.048)	0.769*** (56.915)	0.152*** (12.832)	0.026*** (2.555)	0.982*** (458.010)	0.232*** (15.126)
<b>Panel B: Results for WTI-Brent-Oman oil futures</b>										
	Lagged WTI	Lagged Brent	Lagged Oman	Lagged ECT	$\alpha_i$	$\beta_i$	$\gamma_i$	$\alpha_{i,C}$	$\beta_{i,C}$	$\gamma_{i,C}$
WTInearby	−0.090*** (−3.512)	0.095*** (3.685)	−0.006 (−0.447)	0.488 (1.423)	0.145*** (40.802)	0.862*** (858.152)	0.026*** (7.332)	0.187*** (11.718)	0.949*** (85.184)	0.242*** (8.031)
Brentnearby	0.014 (0.545)	−0.007 (−0.264)	−0.016 (−1.229)	0.815** (2.369)	−0.017*** (−5.905)	0.897*** (878.827)	0.133*** (46.500)	0.078*** (5.247)	0.956*** (96.914)	0.274*** (8.585)
Omannearby	0.034*** (3.295)	0.939*** (89.561)	−0.017*** (−3.060)	−0.418*** (−2.986)	0.359*** (27.987)	0.198*** (106.093)	0.007 (0.538)	−0.047 (−0.843)	0.068 (0.225)	0.232** (2.071)
<b>Panel C: Results for Brent-INE-Oman oil futures</b>										
	Lagged Brent	Lagged INE	Lagged Oman	Lagged ECT	$\alpha_i$	$\beta_i$	$\gamma_i$	$\alpha_{i,C}$	$\beta_{i,C}$	$\gamma_{i,C}$
Brentnearby	0.077*** (2.715)	−0.056** (−1.972)	−0.024 (−1.099)	−1.477*** (−2.596)	−0.020 (−1.007)	0.719*** (29.143)	0.233*** (11.660)	0.095*** (4.949)	−0.497 (−1.153)	0.135* (1.680)
INEnearby	0.084*** (2.983)	−0.025 (−0.899)	−0.023 (−1.106)	−0.899 (−1.602)	0.117*** (9.701)	0.861*** (33.352)	0.008 (0.587)	0.539*** (20.414)	0.227** (2.216)	0.095 (1.040)
Omannearby	0.938*** (76.976)	−0.002 (−0.150)	−0.006 (−0.671)	0.236 (0.970)	0.163 (0.627)	0.663*** (39.831)	0.921*** (3.518)	0.101** (2.503)	0.343 (0.676)	0.711*** (2.953)

Note: This table presents the estimation results of VECM-GJR-GARCH-AG-DCC for extended samples. The mean and volatility models are as follows:

$$\Delta X_t = \alpha\beta'X_{t-1} + \sum_{i=1}^{k-1}\Gamma_i\Delta X_{t-i} + \mu + \varepsilon_t \quad \varepsilon_t \sim N(0, H_t), \quad H_t = D_t R_t D_t,$$

$$D_t = \text{diag}\left(h_t^{1/2}\right), \quad h_{it} = \omega_i + \alpha_i \varepsilon_{i,t-1}^2 + \beta_i h_{i,t-1} + \gamma_i \{\min(\varepsilon_{i,t-1}, 0)\}^2,$$

The correlation estimator  $R_t$  can be written in terms of covariance matrix  $Q_t = (q_{ij,t})$  as  $R_t = (\text{diag}(Q_t))^{-1/2} Q_t (\text{diag}(Q_t))^{-1/2}$ . The evolution of  $Q_t$  is given by:

$$q_{ij,t} = \bar{\rho}_{ij} + \alpha_{i,C}\alpha_{j,C}(\varepsilon_{i,t-1}\varepsilon_{j,t-1} - \bar{\rho}_{ij}) + \beta_{i,C}\beta_{j,C}(q_{ij,t-1} - \bar{\rho}_{ij}) + \gamma_{i,C}\gamma_{j,C}(\eta_{i,t-1}\eta_{j,t-1} - \bar{\rho}_{ij})$$

The  $t$  statistics are reported in parenthesis below the coefficients with \*\* and \*\*\* denoting significance at 5% and 1%, respectively. The sample period is from July 11 to August 21, 2018.

Abbreviations: INE, International Energy Exchange; WTI, West Texas Intermediate.

GJR-GARCH results in Panel A, Oman futures returns exhibit a much higher degree of asymmetric volatility. For the AG-DCC results in Panel A, the estimated coefficient  $\gamma_C$  for Oman return is not significant, which suggests that the correlations between Oman and the other two crude oil futures did not tend to be higher responding to their negative returns. In other words, negative shocks did not increase comovement of Oman futures with other futures markets, which is different from the case of China's crude oil futures. On average, the conditional correlations estimated from the AG-DCC model are 4.5% between WTI and Oman returns and 6.5% between Brent and Oman returns, respectively, much lower than the counterparts between the Chinese and these two major international crude oil futures markets in Table 5.

Panel B of Table 8 presents the estimation results of the GARCH-BEKK model for WTI, Brent, and Oman oil futures. There is one-way dependence of the Oman future volatility on return shocks from WTI futures since  $\alpha_{13}$  is significant. Meanwhile, there is strong bidirectional spillover effect in the intraday volatility between Oman and major

oil futures since all off-diagonal parameters  $b_{ij}$  are statistically significant. However, information linkage of Oman futures with the global market is much weaker than the Chinese futures counterpart. The average conditional correlations from the BEKK models are 4.8% between WTI and Oman returns and 6.9% between Brent and Oman returns, respectively, comparable to those from the AG-DCC models.

In sum, our results in Tables 7 and 8 confirm that during its first 3 months, China's crude oil futures market is better integrated to the world market than Oman futures market in terms of return and volatility linkages.

## 5 | FURTHER ANALYSIS

We extended our sample to the end of August 2018, before the physical delivery in September 2018 for the first Chinese nearby crude oil futures. The additional sample period is from July 11 to August 21, 2018,<sup>10</sup> and we only examine the full sample since it is relatively short. The cointegration tests (not reported here) confirm the existence of one cointegrating vector among all these oil futures markets during the extended period.

**TABLE 10** Results of VECM- GARCH-BEKK Models for extended samples

<b>Panel A: Results for WTI-Brent-INE oil futures</b>										
	<b>Lagged WTI</b>	<b>Lagged Brent</b>	<b>Lagged INE</b>	<b>Lagged ECT</b>	$a_{i1}$	$a_{i2}$	$a_{i3}$	$b_{i1}$	$b_{i2}$	$b_{i3}$
WTInearby	−0.069** (−2.004)	0.123*** (3.358)	−0.039 (−1.875)	0.077 (0.430)	0.703*** (18.150)	0.575*** (23.326)	0.363*** (28.397)	−1.043*** (−16.124)	−1.589*** (−37.118)	−0.972*** (−25.043)
Brentnearby	0.029 (0.887)	0.033 (0.946)	−0.043** (−2.138)	−0.098 (−0.567)	−0.247 (−1.619)	−0.427*** (−3.453)	−0.060 (−0.840)	0.051 (0.726)	0.911*** (15.639)	0.008 (0.218)
INEnearby	−0.024 (−0.644)	0.062 (1.601)	0.031 (1.386)	−0.442** (−2.308)	−0.053*** (−6.126)	−0.012*** (−3.175)	−0.279*** (−20.364)	0.226*** (7.779)	0.192*** (7.832)	1.074*** (73.271)
<b>Panel B: Results for WTI-Brent-Oman Oil Futures</b>										
	<b>Lagged WTI</b>	<b>Lagged Brent</b>	<b>Lagged Oman</b>	<b>Lagged ECT</b>	$a_{i1}$	$a_{i2}$	$a_{i3}$	$b_{i1}$	$b_{i2}$	$b_{i3}$
WTInearby	−0.090*** (−3.509)	0.095*** (3.685)	−0.006 (−0.435)	0.497 (1.447)	−0.326*** (−11.368)	0.002 (0.067)	0.002 (0.134)	0.789*** (11.827)	1.487*** (30.368)	0.022 (1.411)
Brentnearby	0.014 (0.548)	−0.007 (−0.264)	−0.016 (−1.218)	0.823** (2.388)	−0.039 (−1.315)	−0.360*** (−12.901)	0.014 (0.937)	0.136 (1.754)	−0.815*** (−12.010)	−0.016 (−1.057)
Omannearby	0.034*** (3.294)	0.939*** (89.552)	−0.017*** (−3.061)	−0.418*** (−2.986)	0.091 (1.277)	0.051 (0.785)	−0.450*** (−11.264)	0.367 (1.833)	0.429 (2.411)	−0.005 (−0.083)
<b>Panel C: Results for Brent-INE-Oman oil futures</b>										
	<b>Lagged Brent</b>	<b>Lagged INE</b>	<b>Lagged Oman</b>	<b>Lagged ECT</b>	$a_{i1}$	$a_{i2}$	$a_{i3}$	$b_{i1}$	$b_{i2}$	$b_{i3}$
Brentnearby	0.077*** (2.713)	−0.056* (−1.959)	−0.023 (−1.088)	−1.497*** (−2.625)	−0.072** (−2.020)	−0.147*** (−8.964)	0.239*** (16.839)	−1.066*** (−24.289)	−0.909*** (−7.474)	0.035 (1.411)
INEnearby	0.084*** (2.981)	−0.025 (−0.888)	−0.023 (−1.096)	−0.917 (−1.630)	0.030*** (3.042)	0.246*** (40.287)	−0.045*** (−3.707)	0.491 (1.900)	1.179*** (15.855)	0.000 (−0.047)
Omannearby	0.938*** (76.957)	−0.002 (−0.150)	−0.006 (−0.670)	0.236 (0.967)	0.001 (0.016)	0.059 (1.948)	−0.042 (−1.280)	1.155*** (7.784)	0.543*** (3.555)	−0.008 (−0.165)

Note: This table presents the estimation results of VECM-GJR-GARCH for extended samples. The mean and volatility models are as follows:

$$\Delta X_t = \alpha\beta'X_{t-1} + \sum_{i=1}^{k-1}\Gamma_i\Delta X_{t-i} + \mu + \varepsilon_t \varepsilon_t \sim N(0, H_t), H_t = CC' + A(\varepsilon_{t-1}\varepsilon'_{t-1})A' + BH_{t-1}B'$$

The  $t$  statistics are reported in parenthesis below the coefficients with \*\* and \*\*\* denoting significance at 5% and 1%, respectively. The sample period is from July 11 to August 21, 2018.

Abbreviations: INE, International Energy Exchange; WTI, West Texas Intermediate.

Table 9 shows the estimation results of VECM-GJR-GARAH-AG-DCC models for the extended sample. In Panel A for WTI, Brent, and INE futures and Panel B for WTI, Brent, and Oman futures, INE and Oman futures react to deviations from the long-run equilibrium, respectively, while the WTI and Brent futures do not. Except for Oman futures, all asset returns exhibit asymmetric volatilities. Meanwhile, negative shocks tend to make both INE and Oman crude oil futures comove more strongly with the two major crude oil futures markets. In Panel C for Brent, INE, and Oman futures, it is neither INE nor Oman futures but Brent futures that react to deviations from the long-run equilibrium, which is somewhat different from the previous pattern.

Table 10 presents the parameter estimates of VECM-GARCH-BEKK models for the extended sample. In all three panels, the VECM results are consistent with those in Table 9. Specifically, the Brent futures react to deviations from the long-run equilibrium with INE and Oman futures. In Panel A, there is two-way information spillover effect between WTI and INE futures since  $a_{13}$  and  $a_{31}$  are statistically significant. Similarly, there are two-way persistent volatility transmissions between WTI and INE futures, as reflected in the significance of  $b_{13}$  and  $b_{31}$ . In addition,  $a_{32}$  and  $b_{32}$  are significant, suggesting new evidence of information and volatility spillovers from the INE futures to Brent futures. By contrast, the results in Panel B show neither information spillover nor volatility transmission between the Oman and the two major crude oil futures. In Panel C, there is two-way information spillover effect between Brent and INE futures while Oman futures are an information receiver of Brent and INE futures. Meanwhile, there are volatility transmissions from Brent and Oman futures to the INE futures.

From all models in Tables 9 and 10, we find that the average conditional correlations between China's and the two major oil futures are much higher than the Oman counterparts, confirming the previous result China's oil futures have stronger return and volatility linkages with the two international major futures markets than Oman futures market.

## 6 | CONCLUSIONS

We employ various multivariate VECM-MGARCH models to examine return and volatility linkages among the four most actively traded international crude oil futures markets, including WTI, Brent, INE, and Oman crude oil futures markets, with allowance for potential asymmetry in their volatilities and correlations. We document several important new findings on international oil futures market linkages.

In line with Protapadakis and Stoll (1983), there are cointegration relationships among these crude oil futures markets, despite substantial oil quality differences in their underlying asset. The new finding contributes to the debate over whether the international crude oil market has becoming closer to "one great pool," which is always examined using cash market data but not futures market data (see, e.g., Galay, 2019; Plante & Strickler, 2019). Consistent with the perception of their relative informational role, both the INE and Oman futures react to deviations from their long-run equilibrium with the WTI and Brent futures. Somewhat surprisingly, during the first 3 months of China's crude oil futures, their return and volatility linkages with international major crude oil futures markets (WTI and Brent) are already stronger than the linkages between these international major crude oil futures markets and the Oman crude oil futures market in the Middle East, which has been in existence for more than 10 years and often considered a regional crude oil market benchmark in Asia.

Noteworthy, the existence of certain long-run price relationships and significant return and volatility dynamic interactions among China's and two international major crude oil futures markets is an indication of initial success of China's crude oil futures market toward becoming a regional benchmark first and eventually a global benchmark. This is because that crude oil is generally considered a relatively homogenous commodity and the law of one price implies strong crude oil cash price linkages. Given the well-documented evidence for strong price linkages between two major international crude oil futures markets and global cash crude oil markets, lack of international linkages between China' and the two global crude oil futures market would simply indicate that China's oil futures market in its infancy is segmented from the global oil market fundamentals and thus is not possible to be seriously considered as a candidate for either a regional or a global benchmark. The evidence in this study does suggest otherwise. Of course, the existence of international linkages is only necessary but not sufficient for China's oil futures market becoming a regional or global benchmark. Further evidence for certain price leadership of China's oil futures in a largely integrated regional or global crude oil futures market is needed for such a purpose.

<sup>10</sup>High-frequency data in Bloomberg can only be traced back for several months. The data between June 27 and July 10, 2018 were already unavailable in Bloomberg when we updated it in 2019. Meanwhile, there are very few observations of INE futures after August 21, 2018, as it is close to the delivery month.

Interestingly, the linkages between China's and international major crude oil futures markets are also much stronger during the INE overnight trading session than during the INE daytime trading, when WTI and Brent futures markets are in their daytime sessions, which may be a reflection of the important information arrival during WTI and Brent daytime sessions and in line with the fact that trading volume and open interests during the INE overnight session is about four times as much as those during the INE daytime session. Nevertheless, it is interesting to note that the INE return is significant in affecting the returns of WTI and Brent futures only during the INE daytime session but not during its overnight session, which is consistent with relative rates of information production in China during the INE daytime session versus its overnight session.

Finally, China's crude oil futures exhibit stronger asymmetric correlations with international major oil futures markets when compared with the asymmetric correlation between international major oil futures markets, implying its higher vulnerability to negative price shocks from other oil futures markets. Future research may be fruitful to examine other important aspects of China's INE oil futures market, including revisiting the issues under study in this paper when the market is more developed when more INE nearby and more distant futures contracts are actively traded (which is not the case at this time).

## ACKNOWLEDGEMENTS

The authors thank Bob Webb (the editor), an anonymous referee, workshop participants at Xiamen University, Tongji University, and WHU-Otto Beisheim School of Management for their helpful comments, and Zeyun Bei and Leon Sheng for their excellent research assistance. We gratefully acknowledge financial supports from the National Natural Science Foundation of China (71571106, 71871195, and 71988101), the Humanities and Social Sciences grant of the Chinese Ministry of Education (18YJA790121), and Mindu Educational Fund.

## DATA AVAILABILITY STATEMENT

The data that support the findings of this study are available on reasonable request from the corresponding author. The data are not publicly available due to privacy or ethical restrictions. Restrictions apply to the availability of Bloomberg data that were used under license for this study.

## DATA CITATION

Brent, INE, WTI and Oman oil futures markets data]; March 26, 2018 to June 26, 2018; Not publicly available; the data set can be acquired from Bloomberg.

Brent, INE, WTI and Oman oil futures markets data]; July 11 to August 21, 2018; Not publicly available; the data set can be acquired from Bloomberg.

## ORCID

Jian Yang  <http://orcid.org/0000-0002-4073-9796>

Yinggang Zhou  <http://orcid.org/0000-0003-3557-076X>

## REFERENCES

- Andersen, T. G., Bollerslev, T., Diebold, F. X., & Vega, C. (2007). Real-time price discovery in global stock, bond and foreign exchange markets. *Journal of International Economics*, 73, 251–277.
- Anderson, T. G., & Bollerslev, T. (1997). Heterogeneous information arrivals and return volatility dynamics: Uncovering the long-run in high frequency returns. *Journal of Finance*, 52, 975–1005.
- Avramov, D., Chordia, T., & Amit, G. (2006). The impact of trades on daily volatility. *Review of Financial Studies*, 19, 1241–1277.
- Cappiello, L., Engle, R. F., & Sheppard, K. (2006). Asymmetric dynamics in correlations of global equity and bond returns. *Journal of Financial Econometrics*, 4, 537–572.
- Chang, C., AcAleer, M., & Tansuchat, R. (2011). Crude oil hedging strategies using multivariate GARCH. *Energy Economics*, 33, 912–923.
- Elder, J., Miao, H., & Ramahander, S. (2014). Price discovery in crude oil futures. *Energy Economics*, 46, S18–S27.
- Engle, R. F., & Kroner, K. F. (1995). Multivariate simultaneous generalized ARCH. *Econometric Theory*, 11, 122–150.
- Engle, R. F. (2002). Dynamic conditional correlation—A simple class of multivariate GARCH models. *Journal of Business and Economic Statistics*, 20, 339–350.
- Eun, C. S., & Sabherwal, S. (2003). Cross-border listings and price discovery: Evidence from U.S.-listed canadian stocks. *Journal of Finance*, 58, 549–575.
- Fleming, J., Kirby, C., & Ostdiek, B. (1998). Information and volatility linkages in the stock, bond and money markets. *Journal of Financial Economics*, 49, 111–137.

- Fung, H., Leung, G., & Xu, X. (2003). Information flows between the U.S. and China commodity futures trading. *Review of Quantitative Finance and Accounting*, 21, 207–285.
- Fung, H., Liu, Q., & Tse, Y. (2010). The information flow and market efficiency between the US and Chinese aluminum and copper futures markets. *Journal of Futures Markets*, 30, 1192–1209.
- Fung, H., Tse, Y., Yau, J., & Zhao, L. (2013). A leader of the world commodity futures markets in the making? The case of China's commodity futures. *International Review of Financial Analysis*, 27, 103–114.
- Galay, G. (2019). Are crude oil markets cointegrated? Testing the co-movement of weekly crude oil spot prices. *Journal of Commodity Markets*, 16, 100088.
- Glosten, L. R., Jagannathan, R., & Runkle, D. E. (1993). On the relationship between the expected value and the volatility of the nominal excess return on stocks. *Journal of Finance*, 48, 1779–1801.
- Hernandez, M. A., Ashid, R., Lemma, S., & Kuma, T. (2017). Market institutions and price relationships: The case of coffee in the Ethiopian commodity exchange. *American Journal of Agricultural Economics*, 99, 683–704.
- Janzen, J. P., & Adjemian, M. K. (2017). Estimating the location of world wheat price discovery. *American Journal of Agricultural Economics*, 99, 1188–1207.
- Jiang, H., Su, J., Todorova, N., & Roca, E. (2016). Spillovers and directional predictability with a cross quantilogram analysis: The case of U.S. and Chinese agricultural futures. *Journal of Futures Markets*, 36, 1231–1255.
- Johansen, S. (1991). Estimation and hypothesis testing of cointegration vectors in Gaussian vector autoregressive models. *Econometrica*, 59, 1551–1580.
- Johansen, S. (1992). Determination of cointegration rank in the presence of a linear trend. *Oxford Bulletin of Economics and Statistics*, 54, 383–397.
- Kao, C., & Wan, J. (2012). Price discount, inventories and the distortion of WTI benchmark. *Energy Economics*, 34, 117–124.
- Kristoufek, L. (2014). Leverage effect in energy futures. *Energy Economics*, 45, 1–9.
- Li, C., & Hayes, D. J. (2017). Price discovery on the international soybean futures markets: A threshold co-integration approach. *Journal of Futures Markets*, 37, 52–70.
- Lin, S. X., & Tamvakis, M. N. (2001). Spillover effects in energy futures markets. *Energy Economics*, 23, 43–56.
- Liu, W. M., Schultz, E., & Swieringa, J. (2015). Price dynamics in global crude oil markets. *Journal of Futures Markets*, 35, 148–162.
- Miao, H., Ramchander, S., Wang, T., & Yang, J. (2018). The impact of crude oil inventory announcements on prices: Evidence from derivatives markets. *Journal of Futures Markets*, 38, 38–65.
- Plante, M., & Strickler, G. (2019). *Closer to one great pool? Evidence from structural breaks in oil price differentials* (Working Paper 1901). Federal Reserve Bank of Dallas.
- Protopapadakis, A., & Stoll, H. R. (1983). Spot and futures prices and the law of one price. *Journal of Finance*, 38, 1431–1455.
- Ross, S. (1989). Information and volatility: The no-arbitrage Martingale approach to timing and resolution irrelevancy. *Journal of Finance*, 44, 1–17.
- Wang, T., Wu, J., & Yang, J. (2008). Realized volatility and correlation in energy futures markets. *Journal of Futures Markets*, 28, 993–1011.
- Wellenreuther, C., & Voelzke, J. (2019). Speculation and volatility—A time-varying approach applied on Chinese commodity futures markets. *Journal of Futures Markets*, 39, 405–417.
- Yang, J., & Leatham, D. J. (1999). Price discovery in wheat futures markets. *Journal of Agricultural and Applied Economics*, 31, 359–370.
- Yang, J., Zhou, Y., & Wang, Z. (2010). Conditional co-skewness in stock and bond markets: Time series evidence. *Management Science*, 56, 2031–2049.
- Zhao, Y., & Wan, D. (2018). Institutional high frequency trading and price discovery: Evidence from an emerging commodity futures market. *Journal of Futures Markets*, 38, 243–270.

**How to cite this article:** Yang J, Zhou Y. Return and volatility transmission between China's and international crude oil futures markets: A first look. *J Futures Markets*. 2020;40:860–884. <https://doi.org/10.1002/fut.22103>